Lipid discovery enabled by sequence statistics and machine learning

Priya M. Christensen[1], Jonathan Martin[1], Aparna Uppuluri[1], Luke R. Joyce[4], Yahan Wei[5], Ziqiang Guan[6*], Faruck Morcos[1*, 2, 3], and Kelli L. Palmer[1*]

[1]Department of Biological Sciences, University of Texas at Dallas, Richardson, TX 75080, USA
[2]Department of Bioengineering, University of Texas at Dallas, Richardson, TX 75080, USA
[3]Center for Systems Biology, University of Texas at Dallas, Richardson, TX 75080, USA
[4]Department of Immunology and Microbiology, University of Colorado Anschutz Medical Campus, Aurora, CO 80045, USA
[5]School of Podiatric Medicine, University of Texas Rio Grande Valley, Harlingen, TX 78550, USA
[6]Department of Biochemistry, Duke University Medical Center, Durham, NC 27710, USA

August 19, 2024

Abstract

Bacterial membranes are complex and dynamic, arising from an array of evolutionary pressures. One enzyme that alters membrane compositions through covalent lipid modification is MprF. We recently identified that *Streptococcus agalactiae* MprF synthesizes lysyl-phosphatidylglycerol (Lys-PG) from anionic PG, and a novel cationic lipid, lysyl-glucosyl-diacylglycerol (Lys-Glc-DAG), from neutral glycolipid Glc-DAG. This unexpected result prompted us to investigate whether Lys-Glc-DAG occurs in other MprF-containing bacteria, and whether other novel MprF products exist. Here, we studied protein sequence features determining MprF substrate specificity. First, pairwise analyses identified several streptococcal MprFs synthesizing Lys-Glc-DAG. Second, a restricted Boltzmann machine-guided approach led us to discover an entirely new substrate for MprF in *Enterococcus*, diglucosyl-diacylglycerol (Glc_2-DAG), and an expanded set of organisms that modify glycolipid substrates using MprF. Overall, we combined the wealth of available sequence data with machine learning to model evolutionary constraints on MprF sequences across the bacterial domain, thereby identifying a novel cationic lipid.

1 Introduction

Lipids are ubiquitous and diverse group of amphiphathic compounds that are critical for fundamental biological processes, including the formation of cell membranes, protection, and cargo delivery; energy storage; and cell signaling pathways [1]. Chemical modifications to lipids, including changes in fatty acid tails (saturated and unsaturated) [2], modifications of head groups [3], and alterations to lipid charge [4], impact these interactions, as well as the physicochemical properties of membranes. Commonly, bacteria synthesize lipids that are negatively charged or neutral [5]. Some bacteria modify the negatively charged lipids with amino acids to make them positively charged to confer resistance to cationic antimicrobial peptides and cationic antibiotics [6, 7]. The bacterial domain is a rich source of natural lipids that are likely co-evolved for specific interactions with host tissues and other cells, yet the full extent of this chemical diversity remains unexplored. Finding bacteria that possess unique lipids can be useful for biotechnology. For example, natural lipids found in bacteria can be used for drug delivery. A study by [8] used low cytotoxic outer membrane vesicles (OMV) that contained a modified lipopolysaccharide (LPS) to deliver siRNA to targeted cancer cells. This delivery mechanism had success and demonstrates the possibility of using naturally occurring bacterial lipids for future drug delivery processes to eukaryotic cells.

One enzyme responsible for modifying lipids in bacteria is the multiple peptide resistance factor (MprF). MprF modifies lipids through the transfer of amino acids from charged tRNAs to the head group of the anionic

membrane phospholipid, phosphatidylglycerol (PG) [4]. The MprF protein is comprised of two domains: an N-terminal flippase domain responsible for moving aminoacylated lipids from the inner membrane leaflet to the outer leaflet and a C-terminal synthase domain responsible for the aminoacyl transfer from tRNA to lipids [9, 10]. Recently, in *Streptococcus agalactiae* (Group B *Streptococcus*, GBS) it was found that MprF can modify two different substrates with lysine (Lys) – the glycolipid glucosyl-diacylglycerol (Glc-DAG) and the phospholipid, PG [11], generating Lys-Glc-DAG, as well as Lys-PG [11, 12] (Figure 1). An *S. agalactiae mprF* deletion mutant no longer synthesizes Lys-Glc-DAG or Lys-PG and expression of *S. agalactiae mprF* in the heterologous host *Streptococcus mitis* conferred Lys-Glc-DAG and Lys-PG synthesis to *S. mitis* [11]. This was the first time MprF was demonstrated to add lysine onto a neutral glycolipid (Glc-DAG).

The synthesis of Lys-Glc-DAG by *S. agalactiae* MprF illustrated a unique lipid substrate and product by the enzyme that had not been characterized before, highlighting the possibility for further exploration into unknown lipids and lipid substrates by MprF of different bacterial species. We sought to investigate the molecular determinants of enzyme specificity and identify other bacterial species that may have this novel specificity. This investigation led us from the standard methodology of BLASTp queries [13], which are based on single residue amino acid substitution frequencies, to a more modern statistical method called a Restricted Boltzmann Machine (RBM) [14], which captures global statistical patterns within natural sequence data. In this work, we develop a general strategy for combining this high-powered statistical model with lipidomic analysis to discover MprF variants with unique enzymatic activity. This process led us to the discovery of an uncharacterized lipid substrate for MprF, diglucosyl-diacylglycerol (Glc_2-DAG), which is present in several strains identified by the parameters of the statistical model. These models also provide interpretable and actionable information for use in further enzyme characterization, and we show that this application is a useful companion tool for experimental work.

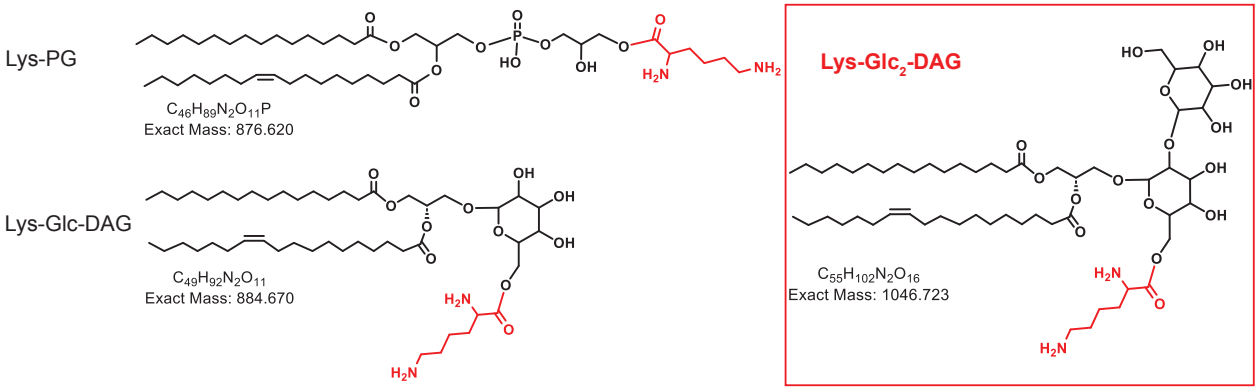

Figure 1: Chemical structures of lysine lipids. Lys-PG, lysyl-phosphatidylglycerol; Lys-Glc-DAG, lysyl-glucosyl-diacylglycerol; Lys-Glc_2-DAG, lysyl-diglucosyl-diacylglycerol.

2 Results

2.1 Simple pairwise sequence statistics identify streptococcal MprF enzymes that synthesize Lys-Glc-DAG

Utilizing a method based on the amino acid sequence of *S. agalactiae* MprF, we identified four streptococcal MprFs with high sequence identity to *S. agalactiae* COH1 MprF (WP_000733236.1). A BLASTp analysis found that *Streptococcus sobrinus* ATCC 27352 MprF (WP_019790557.1) had 61.4% amino acid identity to the *S. agalactiae* MprF, *Streptococcus salivarius* ATCC 7073 MprF (WP_002888893.1) had 43.09% amino acid identity, *Streptococcus ferus* MprF (WP_018030543.1) had 61.88% amino acid identity, and *Streptococcus downei* (WP_002997695.1) had 61.03% amino acid identity (Table 1). Plasmids were designed to express the *S. sobrinus mprF* (pSobrinus), *S. salivarius mprF* (pSalivarius), *S. ferus mprF* (pFerus), and *S. downei mprF* (pDownei) genes. The plasmids were transformed into the expression host *S. mitis* NCTC12261

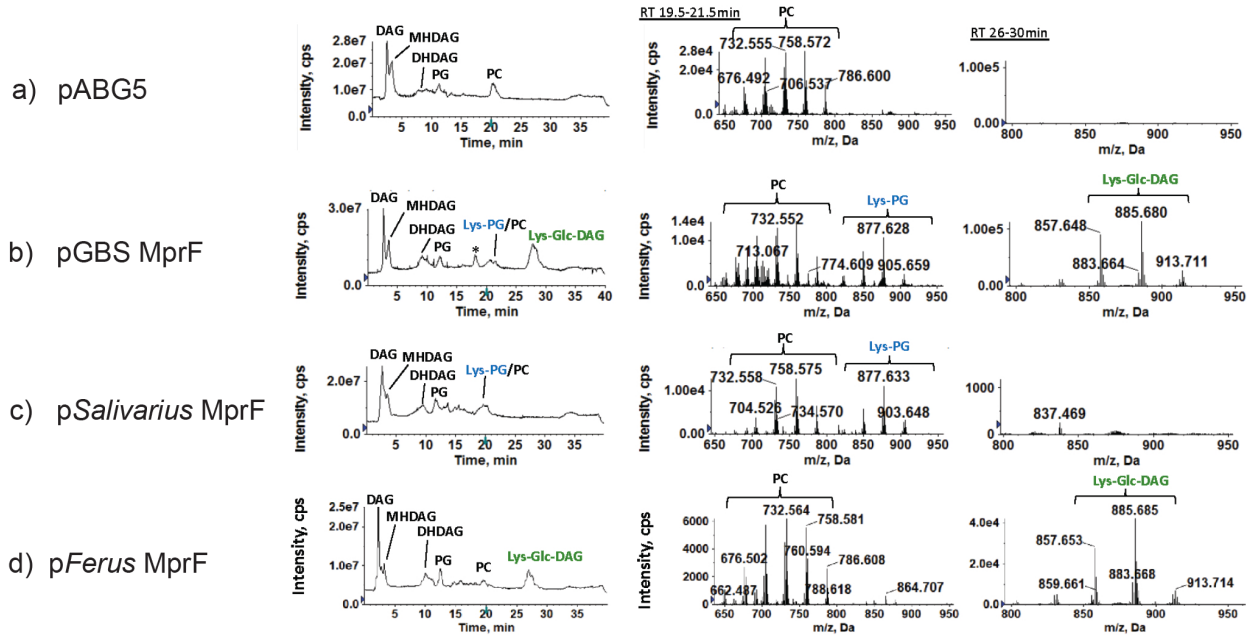

Figure 2: Synthesis of lysine lipids (Lys-PG and Lys-Glc-DAG) in *S. mitis* expressing *mprFs* from *S. agalactiae*, *S. salivarus*, and *S. ferus*. (a) *S. mitis* NCTC12261 with empty vector control (pABG5) lacks lysine lipids; (b) *S. agalactiae mprF* (pGBSMprF) produces both Lys-PG and Lys-Glc-DAG; (c) *S. salivarius mprF* produces only Lys-PG; (d) *S. ferus mprF* produces only Lys-Glc-DAG. Left panels: total ion chromatograms (TIC); middle panels: mass spectra of retention time 19.5–21.5 min showing Lys-PG and PC; right panels: mass spectra of retention time 26–30 min showing Lys-Glc-DAG. Note: "*" is an extraction artifact due to chloroform used. DAG, diacylglycerol; MHDAG, monohexosyldiacylglycerol; DHDAG, dihexosyldiacylglycerol; PG, phosphatidylglycerol; Lys-PG, lysyl-phosphatidylglycerol; Lys-Glc-DAG, lysyl-glucosyl-diacylglycerol; PC, phosphatidylcholine.

(SM61). The empty vector (pABG5Δ*phoZ*, referred to as pABG5 here) was also transformed (Figure 2a). *S. mitis* does not natively encode *mprF* but synthesizes lipids (Glc-DAG; PG) that are substrates for *S. agalactiae* MprF [15, 16, 11], making it an appropriate heterologous host for expressing streptococcal MprFs. Previously, a plasmid expressing *S. agalactiae mprF* (pGBSMprF) [11] was generated and transformed into *S. mitis*. Lys-Glc-DAG and Lys-PG presence in SM61 was only possible with the expression of pGBSMprF (Figure2b) [11].

S. mitis lipids of strains expressing the plasmids pSobrinus (Table 1), pSalivarius (Figure 2c), pFerus (Figure 2d) and pDownei (Table 1) were analyzed. Lipidomic analysis found that pSobrinus, pDownei, and pFerus conferred synthesis of Lys-Glc-DAG, but not Lys-PG in *S. mitis*. Notably, pFerus confers synthesis of Lys-Glc-DAG at a similar level to *S. agalactiae* MprF (Figures 2b, d). In contrast, pSalivarius conferred synthesis of Lys-PG only and not Lys-Glc-DAG. Importantly, *S. salivarius* MprF also synthesized Lys-PG at a level most similar to *S. agalactiae* MprF (Figures 2b, c). Lysine-modified lipids synthesized by *S. mitis* strains expressing streptococcal MprFs used in this study are summarized in Table 1. In general, streptococcal MprF enzymes with higher amino acid percent (> 60%) to *S. agalactiae* MprF conferred Lys-Glc-DAG synthesis to *S. mitis*, but only *S. agalactiae* MprF conferred both Lys-Glc-DAG and Lys-PG synthesis in *S. mitis*.

Bacteria Strains	% Amino Acid Identity (Similarity)	Lys-PG	Lys-Glc-DAG
SM61(pGBSMprF)	100.0 (100.0)	✓	✓
SM61(pFerus)	61.9 (79.0)	X	✓
SM61(pSobrinus)	61.4 (79.0)	X	✓
SM61(pDownei)	61.0 (79.0)	X	✓
SM61(pSalivarius)	43.1 (66.0)	✓	X
SM61(pABG5)	- (-)	X	X

Table 1: **Summary of different MprF variants expressed in *S. mitis* and the lysine lipids they produce**. Percentage of amino acid identity and similarity compared to *S. agalactiae* COH1 MprF; data obtained from BLASTp. The lipids each strain synthesize are denoted by a checkmark or an x. Lys-PG, lysyl-phosphatidylglycerol; Lys-Glc-DAG, lysyl-glycosyl-diacylglycerol.

2.2 Restricted Boltzmann Machines can provide sensitive, rational guidance for sequence classification

We set out to understand which specific MprF amino acid residues are involved in enzyme specificity for either the PG or Glc-DAG substrate. To this end, we employed a Restricted Boltzmann Machine (RBM), a probabilistic graphical model which aims to model the probability of data in a data set through statistical connections between the features of the data and a set of hidden units. [17]. This class of models is closely related to another model termed the Boltzmann Machine. The Boltzmann machine formulation is closely related to the Potts model from physics, which was successfully applied in biology to elucidate important residues in protein structure and function [18], one example being the careful tuning of enzyme specificity in bacterial two-component regulatory systems [19, 20]. The Boltzmann Machine formulation from [18], termed Direct-Coupling Analysis (DCA), stores patterns in the form of a pairwise coupling matrix and local field matrix (shown in Equation 2), which has been useful in understanding how likely pairs of residues are to interact in physical space. We hypothesize that *S. agalactiae* MprF and other MprF enzymes that utilize glycolipid substrates have unique patterns of interacting residues relative to those enzymes that use only PG as a substrate.

While modeling how pairs of residues covary is powerful, many important features of enzyme function like allostery or enzyme specificity (which is the purpose of this analysis) may involve more than two residues [21], and in these situations it can be difficult to connect sets of residues using solely pairwise parameters [22]. Therefore, a more global approach is required to address our hypothesis. To this end, a RBM has recently been developed for use in the learning of protein sequence data, with special attention given to producing a model which produces sparse, interpretable, and biologically meaningful representations of these higher-order statistical couplings within the hidden units [14]. The design of this RBM can be seen in Figure 3, where the model architecture is represented by purple dots and green triangles. The dots are the "visible" layer, which take in input sequences and encode them into the "hidden" layer, where each triangle represents a separate hidden unit. The lines connecting the visible and hidden layers show that each hidden unit can see all the visible units (the statistics are global), but they cannot see any of the other hidden units, meaning the hidden units are mutually independent. This global model with mutually independent hidden units (see the marginal distribution form shown in Equation 3) allows the following useful properties: higher-order couplings between residues (sets of coupled residues instead of pairs); bimodal hidden unit outputs given the training data set (Equation 4); sparse, interpretable configurations of the hidden units (w_μ) (Equation 5) and a compositional representation of the hidden unit weights [23], where input sequences are modeled largely through combinations of hidden units instead of single, highly activating units.

The compositional representation is a critical feature of this method, allowing us to find independently coupled sets of residues which in combination describe these protein sequences, and it is achieved through the particular choices of training parameters. More details on the training parameter choices are found in

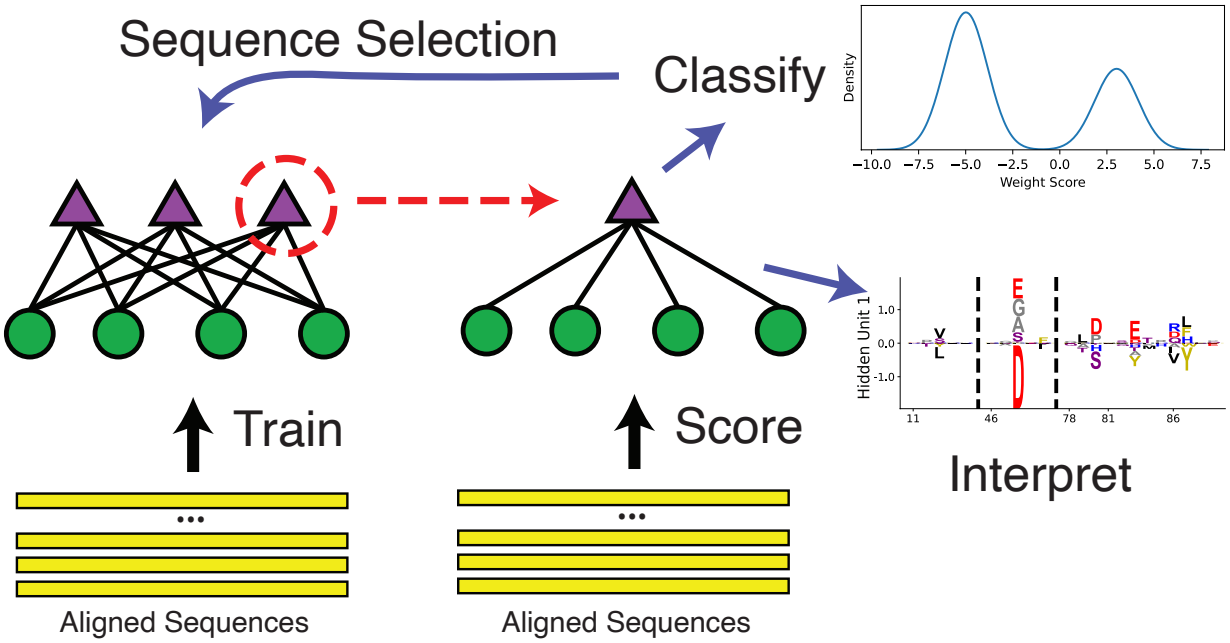

Figure 3: Schematic of the RBM methodology. An aligned set of protein sequences is first used to learn a hidden unit representation that best describes the statistics of the sequence dataset given restrictions on the hidden unit representation. Then, the individual hidden units can be studied to find particular units which allow useful enzyme classification, and additionally, these weights can be meaningfully interpreted as statistically co-varying sequence configurations. Additionally, the classification can be used to create filtered datasets to train more models.

Methods and Materials. In particular, we focus on the scoring of sequences using individual hidden units w_μ:

$$I_\mu(\mathbf{v}) = \sum_i \mathbf{w}_{i\mu}(\mathbf{v}_i) \tag{1}$$

where $\mathbf{v}$ is an input sequence vectorized through one-hot encoding, to produce a hidden unit activation (a single number) which depends on the input sequence residues at position i and the value of the hidden unit weight matrix for that residue at that position.

We used this methodology to study the sequences in the family of MprF, which is a large protein composed of independent flippase and synthase domains [9, 24]. In our analysis, we restrict ourselves to the cytosolic region (see yellow box in Figure 4a), also known as the aminoacyl-PG synthase domain, which constituted the Pfam family DUF2156 (now renamed LPG_synthase_C) [25]. One hidden unit in particular is highlighted, where we find bimodal activation (Figure 4b) of the hidden unit (Figure 4c) when Equation 1 is evaluated with the training sequences. Interpreting the sequence histograms, a positive value activation in Figure 4b corresponds to a sequence containing combinations of the residues listed in the positive portion of the weight diagram in Figure 4c, whereas a negative activation corresponds to residues in the negative portion. For display purposes, the residue weights shown in all of our hidden units correspond to the positions where the magnitude of the visible positions $w_{i\mu}$ are greater than some threshold proportional to the largest magnitude position (position 212); the hidden units has values for all possible amino acids in the entire protein length, but they are considerably smaller than this threshold and generally very low.

Two positions in particular, 152 and 212, in the positive portion of the hidden unit correspond to residues 684 and 742, which were experimentally demonstrated to be relevant for aminoacylated-PG production by the *Bacillus licheniformis* and *Pseudomonas aeruginosa* cytosolic synthase domain variants [26]; in *B. licheniformis* the residues which form a complex with the lysine from Lys-tRNA^{Lys} are shown in Figure 4c. We have highlighted these two aforementioned variants as well as the *S. agalactiae* variant for demonstration

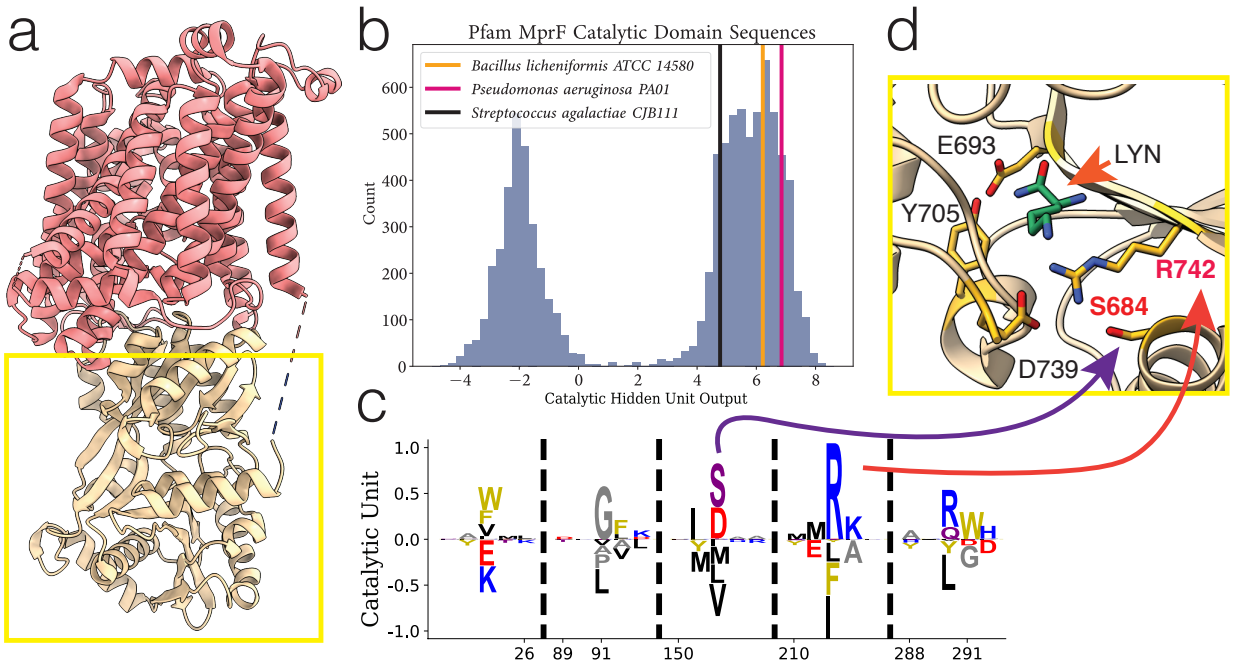

Figure 4: Example of hidden unit analysis and usage. (a) The structure of PDB:7DUW, with the red colored region being the transmembrane flippase domain and the yellow boxed region the cytosolic domain which we focus on. (b) The activations produced by inputting a sequence into a hidden unit, producing a single number as output which corresponds to a summation of negatively and positively weighted residues. Performed on entire training set (histogram in blue), highlighting sequences corresponding to predominantly positive weighted residues. (c) Hidden unit from an RBM trained on the Pfam DUF2156 domain. The MSA positions 152 and 212 correspond to residues S684 and R742, respectively. (d) Residues (in yellow) in the MprF cytosolic domain which form the binding pocket for Lys-tRNA^{Lys} (the ligand analogue L-lysine amide shown in green), from PDB:4V36. LYN, L-lysine amide.

of sequence scoring through Equation 1 in Figure 4a. We used this hidden unit to create a filtered data set; only sequences that contained this necessary motif were of interest to us, and we subsequently trained a new model using only sequences with a catalytic hidden unit activation greater than 2 (because it cleanly split the bimodal distribution). We outline this general workflow in Figure 3. We also note that the full length sequences of the sequences included in our new dataset are enriched with sequences which contain the bacterial flippase domain (shown in red in Figure 4a), and the sequences we removed rarely contain the flippase domain (see Figure S2 for domain analysis).

2.3 RBM hidden units identify plausible sequence residues for functional characterization

After filtering the data set and training another model, we set out to find hidden units which could describe MprF specificity. To this end, we identify hidden units which are sparse, have high overall magnitude, and involve residues which could be plausibly linked to the lipid binding specificity (see Methods for more details). Through this search method we identified the two hidden units shown in Figure 5a. They both have high sparsity and high magnitude relative to the majority of other hidden units in the model, and importantly they correspond to residues localized to regions of the catalytic domain that had been previously identified through Autodock experiments using a PG molecule with side chains C5:0/C8:0 [26] (highlighted in Figure 5a). The scoring of the training set of sequences with these hidden units is shown in Figure 5b, and we see a clear separation between the cytosolic domain sequences which produces Lys-Glc-DAG (from *S. agalactiae*) and two domain variants which produce only aminoacylated-PG (from *P. aeruginosa* and *B. licheniformis*). Importantly, these output activations depend on a greatly reduced subset of the full sequence and do not correspond to clustering on total sequence identity (Figure S1).

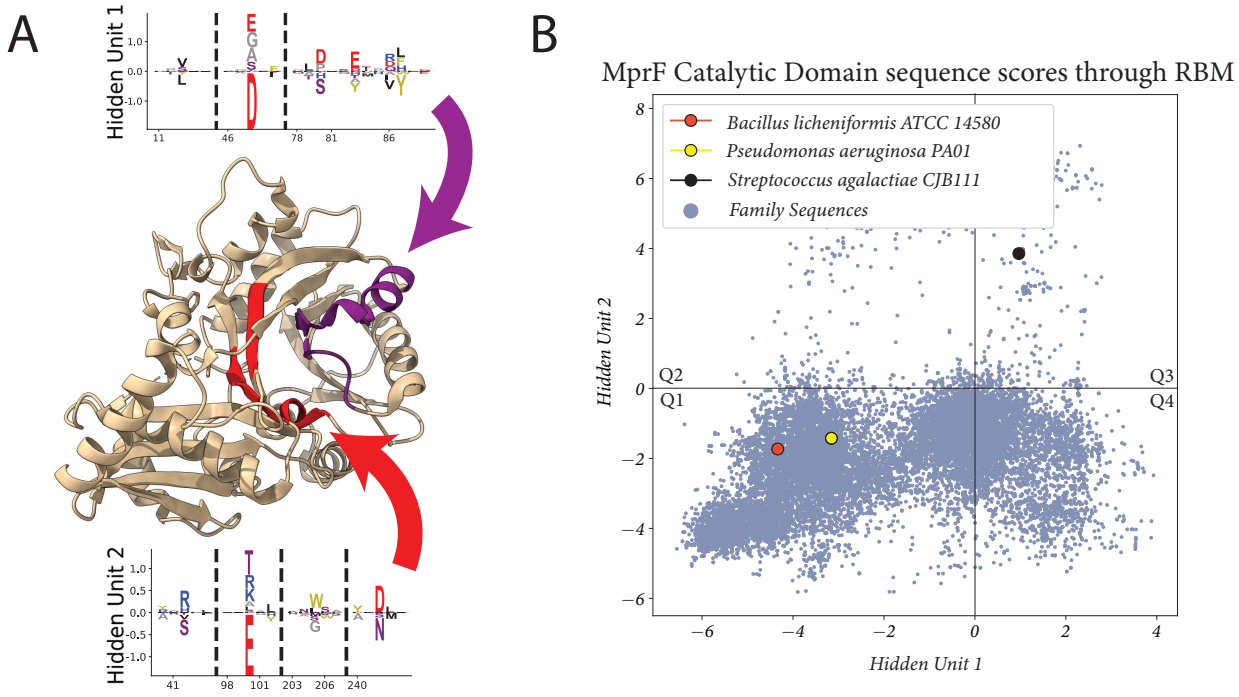

Figure 5: Proposed set of hidden units for classifying lipid specificity. (a) two hidden units found in an RBM trained on the filtered Pfam dataset. The hidden unit residues are highlighted in the PDB:4V34 structure, with arrows pointing to their corresponding residue sets. (b) the activations of the hidden units when scoring the sequences used in the training set and sequences from NCBI not used during training (N=23,138). *S. agalactiae* produces Lys-Glc-DAG and Lys-PG, while *B. licheniformis* and *P. aeruginosa* produces only aminoacylated-PG. Q1-Q4 are quadrant labels which we refer to throughout the paper.

Using these two hidden units as sequence classifiers with a potential link to the substrate specificity of cytosolic domain variants, we used Figure 5b to propose sequences in quadrant three (Q3), the quadrant occupied by the *S. agalactiae* MprF variant with this novel glycolipid-modifying function. We selected a sequence which was distant in terms of sequence identity from the *Streptococcus* genus (Table S1) and which has been implicated in human pathologies [27], *Enterococcus dispar* MprF. We also emphasize that the two hidden units we selected are from a set of 300 total hidden units, and that while other hidden units may differentially classify our three sequences, without the additional link to lipid binding provided by the Autodocking experiment there would be only weak justification for using their activations to make predictions.

2.4 Enterococcal MprF enzymes synthesize Lys-Glc-DAG, Lys-PG, and a novel cationic glycolipid Lys-Glc$_2$-DAG

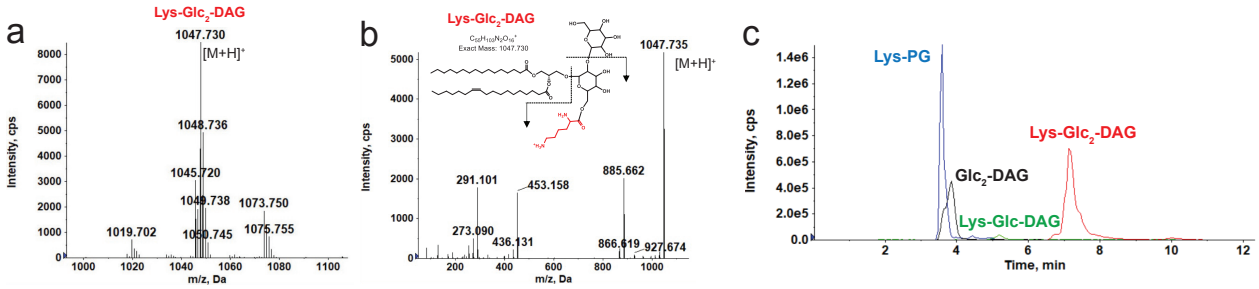

Figure 6: Identification of Lys-Glc$_2$-DAG in *E. dispar*. (a) Positive ion mass spectrum of Lys-Glc$_2$-DAG species in *E. dispar*. Major Lys-Glc$_2$-DAG species with carbon atoms (before colon) and double bonds (after colon) (b) MS/MS product ions and fragmentation scheme of the most abundant Lys-Glc$_2$-DAG ion at m/z 1047.73. (c) Extracted ion chromatograms of LC/MS of lysine lipids (Lys-PG, Lys-Glc-DAG, Lys-Glc$_2$-DAG) and Glc$_2$-DAG separated on an amino HPLC column. Glc$_2$-DAG, diglucosyl-diacylglycerol; Lys-PG, lysyl-phosphatidylglycerol; Lys-Glc-DAG, lysyl-glucosyl-diacylgylcerol; Lys-Glc$_2$-DAG, lysyl-diglucosyl-diacylglycerol.

Enterococcus dispar ATCC 51266 was identified as a possible candidate for novel lipid synthesis through the analyses described above. Remarkably, our lipidomic analysis found that *E. dispar* synthesizes a novel cationic lipid, lysyl-diglucosyl(Glc$_2$)-diacylglycerol (Lys-Glc$_2$-DAG) (Figure 1, Figure 6a,b), as well as Lys-Glc-DAG and Lys-PG (Figure 6c, Figure S3). The structural identification of Lys-Glc-$_2$-DAG was supported by exact mass measurement ($[M+H]^+$ observed at m/z 1047.730; calculated m/z 1047.731) and tandem MS (Figure 6b). Lys-Glc-$_2$-DAG is unusually polar and charged for a lipid; chromatographically, Lys-Glc$_2$-DAG is highly retentive on a silica-based normal phase column and elutes off the column at the very end of the gradient (Figure S3). The use of an amino-based HPLC column led to much improved elution profiles for Lys-Glc$_2$-DAG and other glyco- and lysine lipids (Figure 6).

The discovery of Lys-Glc$_2$-DAG in *Enterococcus dispar* led us to analyze other *Enterococcus* strains: *E. faecium* 1,231,410, *E. faecalis* T11 and OG1RF *E. gallinarium* EG2, *E. casseliflavus* EC10, and *E. raffinosus* Er676. All *Enterococcus* strains examined were found to synthesize Lys-PG, Lys-Glc-DAG and Lys-Glc$_2$-DAG at varying levels (Figure 7a and Table 2). MprF-dependent Lys-PG production by *E.faecalis* and *E. faecium* was previously reported [28, 29], but cationic glycolipids production has not been previously reported. *E. gallinarium* EG2 and *E. casseliflavus* EC10 encode a single copy of *mprF* gene, while the other enterococci we tested encode two distinct *mprF* genes (*mprF*1 and *mprF*2) [28, 29]. When these MprF sequence variants are plotted using our chosen RBM hidden units, we see that the two single copy strains plot in quadrant two (Q2), while for the two copy sequences, each MprF variant maps to separate coordinates (Figure S4). Both *E. raffinosus* Er676 MprF variants plot to quadrant two (with the lowest Weight 2 value being 0.34). The *E. faecium* and *E. faecalis* variants have copies plotting directly in quadrant one and variants plotting farther out from the sequence cluster; we note that the two displaced variants are both lacking the characteristic aspartic acid and glutamic acid amino acids at positions 100 and 48 in the hidden units (Figure 5a), which are the dominant contributions for determining quadrant one occupancy.

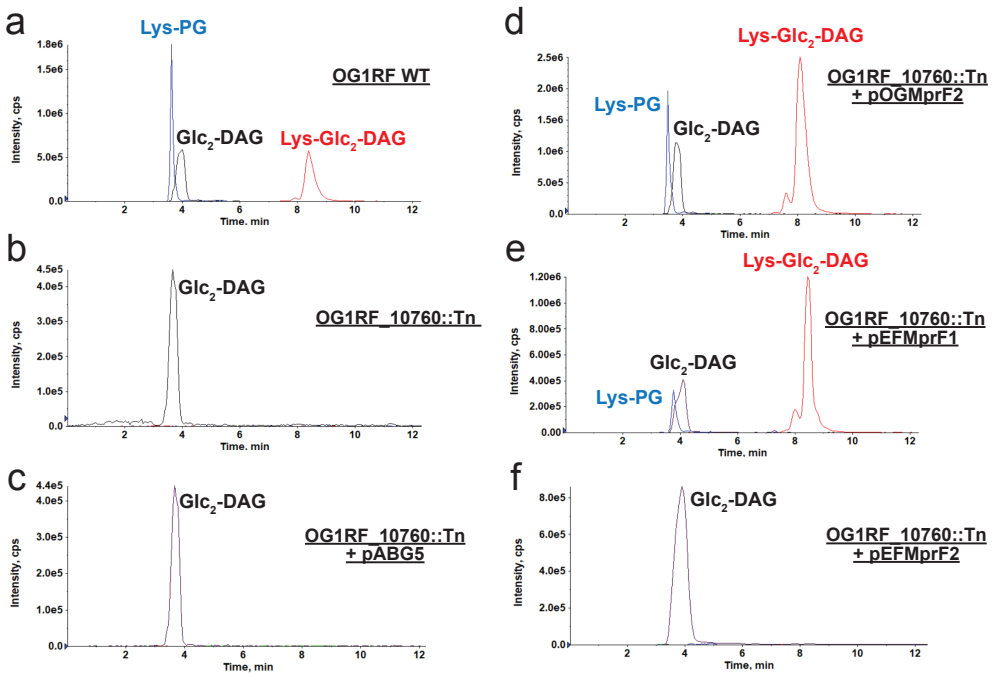

Figure 7: *E. faecalis* MprF2 and *E. faecium* MprF1 confer Lys-Glc$_2$-DAG synthesis. (a) OG1RF-WT; (b) OG1RF_10760::Tn lacks lysine lipids; (c) OG1RF_10760::Tn + pABG5 lacks lysine lipids; (d) OG1RF_10760::Tn + pOGMprF2 restores lysine lipids; (e) OG1RF_10760::Tn + pEFMprF1 restores lysine lipids; (f) OG1RF_10760::Tn + pEFMprF2 lacks lysine lipids. Expression of OGMprF2 and EFMprF1 in OG1RF_10760 Tn mutant restore Lys-Glc$_2$-DAG synthesis. Shown are the extracted ion chromatograms of lysine lipids (Lys-PG, Lys-Glc$_2$-DAG) and Glc$_2$-DAG separated on an amino HPLC column. Note: Lys-Glc-DAG was found in trace amounts or missing from lipid extractions. Glc$_2$-DAG, diglucosyl-diacylglycerol; Lys-PG, lysyl-phosphatidylglycerol; Lys-Glc$_2$-DAG, lysyl-diglucosyl-diacylglycerol.

To clarify which variants were determinants of the novel cationic lipid production, lipidomic analysis on an *E. faecalis* OG1RF mini-mariner (EfaMarTn) transposon mutant [30] with a transposon insertion within OG1RF_10760 *mprF* (referred to as *mprF*2 in previous studies [28]; OG1RF_10760::Tn) revealed that Lys-PG, Lys-Glc-DAG and the newly identified Lys-Glc$_2$-DAG were absent when the synthase domain of the gene was disrupted (Figure 7b, Table S1). This led us to the conclusion that *E. faecalis mprF*2 is necessary for the synthesis of the three Lys-lipids in *E. faecalis*. When the empty vector (pABG5) was transformed into OG1RF_10760::Tn, no Lys-lipids synthesis was observed as expected (Figure 7c). This phenotype was complemented by expression of *E. faecalis mprF*2 from a plasmid (pOGMprF2) (Figure 7d). Additionally, expression of *E. faecium mprF1* (EFTG_00601) (pEfMprF1) restored Lys-PG and Lys-Glc$_2$-DAG synthesis to the *E. faecalis* OG1RF_10760::Tn strain (Figure 7e), while *E. faecium mprF2* (EFTG_02430) did not rescue Lys-lipid synthesis (Figure 7f). Taken together, these data indicate that *E. faecalis* MprF2 (OG1RF_10760) and *E. faecium* MprF1 (EFTG_00601), like *S. agalactiae* MprF, act on both phospholipid and glycolipids substrates, additionally synthesizing the novel cationic glycolipid, Lys-Glc$_2$-DAG.

2.5 Hidden unit 2 is correlated with Glc$_N$-DAG substrate activity in MprF

When we started our RBM analysis, we had substrate specificity information for only the quadrants one and three, and through identifying the novel substrate in *E. dispar* we expanded our testing to quadrant two by testing *Enterococcus* strains. To expand our RBM analysis, we tested specific sequences which were found in quadrant four (Q4). We conducted lipid analysis on *Ligilactobacillus salivarius* ATCC 11741, *Levilactobacillus brevis* ATCC 14869, *Lacticaseibacillus rhamnosus* ATCC 7469, *Lactobacillus casei* ATCC 393, and *Lacticaseibacillus paracasei* ATCC 25302. All strains tested synthesize Lys-PG (Table 2). Only *Levilactobacillus brevis* and *Lacticaseibacillus paracasei* synthesized Lys-Glc$_2$-DAG, *L. paracasei* synthesized

low levels of Lys-Glc$_2$-DAG. An additional quadrant one (Q1) strain *Exiguobacterium acetylicum* UTDF19-27C, was analyzed by lipidomics. It was found to synthesize only Lys-PG. This MprF falls near *Staphylococcus aureus* RN4220 and *Bacillus subtilis* 168 in our plot, both of which synthesize only Lys-PG [31, 24] (and experimentally confirmed in this study). This further supports that strains located in quadrant one of Figure 8 are capable of Lys-PG synthesis.

Summaries of all functional species/variants tested and the Lys-lipids they produced are shown in Table 2, and plotted in the two RBM hidden units in Figure 8. We list for each MprF variant which of the three tested lipids it acts on, and in Figure 8 we indicate whether a variant has only PG as a substrate or if it operates on Glc$_N$-DAG as a substrate irrespective of its PG activity. With this plot, we can see that sequences which plot with positive activations in hidden unit 2 are more likely to have Glc$_N$-DAG as a substrate (8/9), and sequences with negative values predominantly use PG (7/11), with a Fisher's exact test p-value of 0.028 (Table S2). Hidden unit 1, however, is not correlated with Glc$_N$-DAG specificity, with a Fisher's exact p-value of 0.67. Therefore we conclude that hidden unit 2, and thus the high magnitude sequence positions identified by it, are correlated with Glc$_N$-DAG specificity.

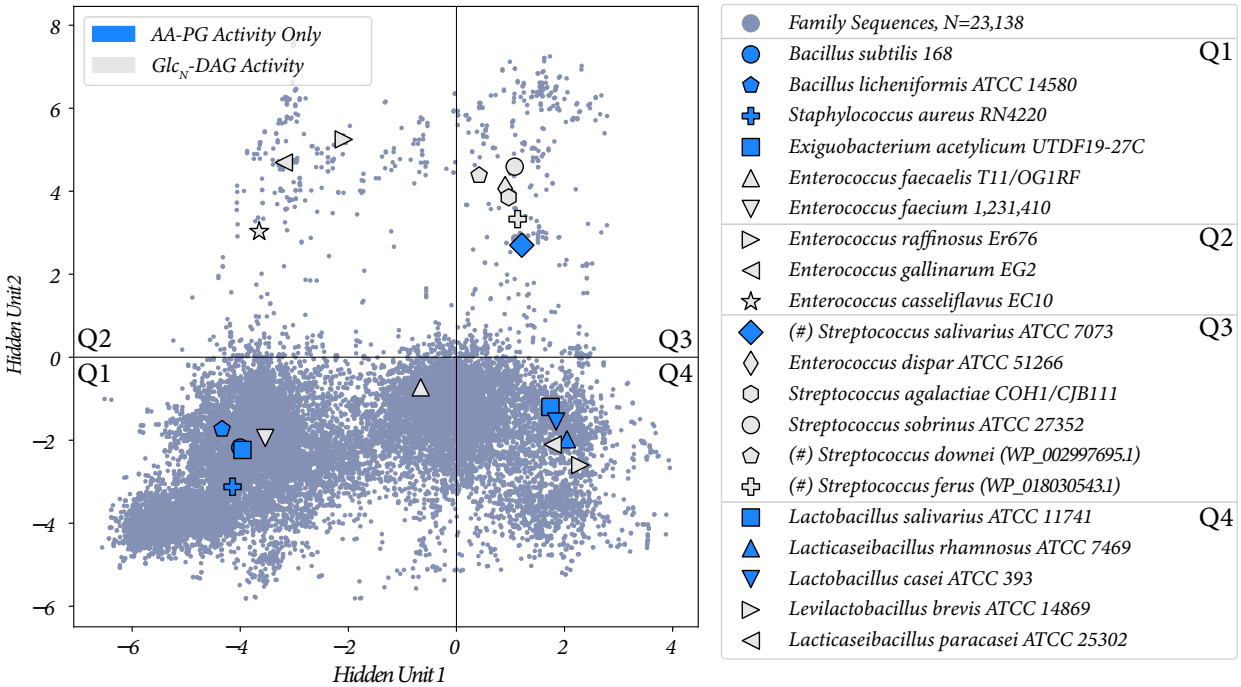

Figure 8: The two proposed hidden unit activations with all of the sequences from Table 2 labeled. Protein ID of highlighted sequences are listed in Table S1. (#) indicates the lipid activity was confirmed through heterologous expression.

3 Discussion

The utilization of the *S. agalactiae* MprF amino acid sequence as a query for BLASTp was a simple method to identify various streptococcal MprFs and further our understanding of MprF specificity. This allowed us to identify three MprFs that can synthesize the highly cationic Lys-Glc-DAG. Importantly, although highly similar to *S. agalactiae* MprF, this method did not identify other streptococcal MprFs capable of lysine addition to both glycolipid and phospholipid substrates (generating Lys-Glc-DAG and Lys-PG) nor did it lead to the identification of a novel cationic glycolipid found in *Enterococcus*. Sequence logos [32] may identify important sequence features, but largely in instances where amino acids are highly conserved. When amino acids must interact to produce a specific function, yet the exact identity of those amino acids is not a requirement, methods which model the strength of amino acid coevolution in sequence sets can find important

	Bacterial Strains	Lys-Glc-DAG	Lys-Glc$_2$-DAG	Lys-PG
Q1	***Bacillus subtilis*** 168	X	X	✓
	Bacillus licheniformis ATCC 14580	X	X	✓
	Staphylococcus aureus RN4220	X	X	✓
	Exiguobacterium acetylicum UTDF19-27C	X	X	✓
	Enterococcus faecalis T11/OG1RF**	✓	✓	✓
	Enterococcus faecium 1,231,410	✓	✓	✓
Q2	***Enterococcus raffinosus*** Er676	✓	✓	✓
	Enterococcus gallinarum EG2	✓	✓	✓
	Enterococcus casseliflavus EC10	✓	✓	✓
Q3	***Streptococcus salivarius**** ATCC 7073	X	X	✓
	Enterococcus dispar ATCC 51266	✓	✓	✓
	Streptococcus agalactiae CJB111/COH1	✓	X	✓
	Streptococcus sobrinus* ATCC 27352	✓	X	X
	Streptococcus downei* (WP_002997695.1)	✓	X	X
	Streptococcus ferus* (WP_018030543.1)	✓	X	X
Q4	***Ligilactobacillus salivarius*** ATCC 11741	X	X	✓
	Lacticaseibacillus rhamnosus ATCC 7469	X	X	✓
	Lactobacillus casei ATCC 393	X	X	✓
	Levilactobacillus brevis ATCC 14869	X	✓	✓
	Lacticaseibacillus paracasei ATCC 25302	X	✓	✓

Table 2: **Table of all strains studied, the quadrant they occupy, and the lipids they synthesize.** ** trace amounts Lys-Glc-DAG present in lipid extractions. * indicates heterologous expression of *mprF* in *Streptococcus mitis*. Lys-Glc-DAG, lysyl-glucosyl-diacylglycerol; Lys-Glc$_2$-DAG, lysyl-diglucosyl-diacylglycerol; Lys-PG, lysyl-phosphatidylglycerol.

signals which in the sequence logo might appear to be negligible. For this reason we used the Restricted Boltzmann Machines (RBM) method [14], which can model statistical connectivity of residues at multiple sites in the protein sequence.

The RBM can be used in a number of ways to study sequence data. Firstly, it allowed us to filter the sequence data using hidden units (Figure 4); the two hidden units which formed the basis of our specificity analysis were not found in models trained on the Pfam dataset when it was initially pulled from Pfam, and this was potentially due to the presence of sequences without relevant catalytic function adding noise to the dataset. The most prominent feature for our purposes is the ability to use the hidden units learned through RBM training to classify sequences. The bimodal nature of this particular model provides a relatively simple interpretation which is straightforward to use for prediction. We show in Figure 5 that the combination of clustering and interpretable hidden unit structure allows us to identify a small subset of residues within a structure, grounding our statistical clustering in MprF's structural features. The combination of experimental evidence and evolutionary information provided a strong rationale for selecting organisms for further study, ultimately leading to the discovery of novel cationic lipid biosynthesis in *Enterococcus dispar* (Figure 6, Figure S3).

One goal of this study was to find the structural determinants of Glc$_N$-DAG activity by MprF, and we found that hidden unit 2 from our RBM analysis was predictive of this. However, there are notable exceptions such as the *E. faecium* allele EGTF_00601, which has sequence features placing it in quadrant one yet has Glc$_N$-DAG activity. Therefore, identifying the exact sequence determinants of Glc$_N$-DAG specificity remains to be fully elucidated. One explanation could be our exclusion of the N-terminal flippase domain and the

non-cytosolic region of the C-terminal domain in the RBM analysis, where important residue interactions determining specificity could occur and is under further investigation. Additionally, a challenge in experimental validation will be to standardize the method of studying *mprF* alleles from diverse organisms. When using native organisms, lipids produced may vary during the growth phase of the organisms, the media they are grown in, and whether a membrane stressor is present (i.e. inducible production of specific lipids). For this study we used stationary phase cultures of equal volume and bacteria were grown in their respective standard laboratory media. The use of a heterologous host for expression of *mprF* alleles is a method of standardization, but may result in not identifying novel lipids that would be found in their native bacteria since the appropriate lipid substrates may not be present [16, 12]. A combination of both approaches (native organisms and heterologous hosts) may be required. Additionally, spike-in controls might be implemented to help us to more quantitatively understand the output specificity of these MprF variants. Ultimately, mutational studies of the residues identified by the RBM will allow for identification of the residues critical for specificity, though likely the residues will depend in part on the primary sequence being altered.

The general method of RBM-guided exploration has applications in enzyme design, for example, in enhancing methods like directed evolution [33]. Concretely, the residues identified through hidden units can be thought of as templates for mutational exploration, greatly reducing the search space for assessing which residues are critical for specificity determination. Enzymes like MprF that produce lipids of modified charge have potential applications in biotechnology and therapeutics, where the design of lipid nanoparticles with different charge and chemical properties of the head group have important physiological implications [34]. Notably, the identification of Lys-Glc$_2$-DAG opens new research avenues, particularly in the fields of antibiotic resistance and host-pathogen interactions, wherein lipid modification and cationic lipids play key roles. With respect to human health, it would be relevant to investigate whether Lys-Glc$_2$-DAG plays a role in enterococcal resistance to the last-line membrane-active antibiotic, daptomycin.

4 Methods and Materials

4.1 Bacterial Strains and Growth Conditions

See Tables S1 and S3 for a full list of bacterial strains used in this study. *Streptococcus mitis* NCTC12261 (referred to as SM61 here) [35] was grown in Todd Hewitt Broth (THB) at 37°C with 5% CO_2. *Escherichia coli* DH5α [36] and *Bacillus subtilis* 168 [37] was grown at 37°C with shaking at 225 rpm in lysogeny broth (LB). *Staphylococcus aureus* RN4220 [38] was grown at 37°C with shaking at 220 rpm in Trypic Soy Broth (TSB). *Streptococcus agalactiae* COH1 ATCC BAA-1176 [39] and CJB111 [40, 41] were grown in THB at 37 °C. *Enterococcus faecium* 1,231,410 [42], *Enterococcus faecalis* T11 [43] and OG1RF [44], *Enterococcus gallinarium* EG2 [42], *Enterococcus casseliflavus* EC10 [42], and *Enterococcus raffinosus* Er676 [45] were grown at 37°C in Brain Heart Infusion (BHI). *Enterococcus dispar* ATCC 51266 [46] was grown at 30°C in BHI. *Exiguobacterium acetylicum* UTDF19-27C was grown in BHI at 37 °C. *Ligilactobacillus salivarius* ATCC 11741 [47], *Lacticaseibacillus rhamnosus* ATCC 7469 [48], *Lactobacillus casei* ATCC 393 [49] and *Lacticaseibacillus paracasei* ATCC 25302 [48] were grown in Lactobacilli MRS Broth at 37°C and 5% CO_2. *Levilactobacillus brevis* ATCC 14869 [50] was grown in Lactobacilli MRS Broth at 30°C, 5% CO_2. *Bacillus licheniformis* ATCC 14580 was grown in nutrient broth at 37°C with shaking at 225 rpm [51]. A transposon mutant of *E. faecalis* OG1RF from [30] with a mini mariner transposon (EfaMarTn) insertion in OG1RF_10760 (OG1RF_10760::Tn) was grown on BHI supplemented with chloramphenicol at a concentration of 15 μ/mL. The mutant was confirmed to be erythromycin-sensitive. The transposon mutant location was confirmed through Sanger sequencing performed by the Genome Center at the University of Texas at Dallas (Richardson, TX).

Where appropriate for plasmid selection, kanamycin (Sigma-Aldrich) was added. For *E. coli*, a concentration of 50 μg/mL was used, for *S. mitis* a concentration of 300 μg/mL, and for *E. faecalis* a concentration of 500 μg/mL was used.

4.2 Routine Molecular Biology Procedures

Genomic DNA was extracted as done previously in [52] and [53]. All PCR reactions used Phusion polymerase (Thermo Fisher Scientific) and Phusion 5x HF buffer (Thermo Fisher Scientific) in a Veriti PCR machine (Applied Biosystems). List of primers used are found in Table S4. Gibson assemblies were completed using a 2x HI-FI Assembly master mix following the manufacturer's protocol (New England Biolabs). PCR clean-up was done using the GeneJET PCR Purification Kit (Thermo Fisher Scientific) per manufacturer protocol. Plasmid extractions were performed per manufacturer protocol using the GeneJET Plasmid miniprep kit (Thermo Fisher Scientific). All plasmid constructs were confirmed by Sanger sequencing at the Massachusetts General Hospital CCIB DNA Core facility or by Illumina sequence at SeqCenter. DNA concentrations were measured using Nanodrop (Thermo Fisher Scientific) or Quibit 2.0 (Invitrogen by Life Technologies). Optical Density at 600 nm (OD_{600nm}) was measured in a disposable cuvette (Thermo Fisher Scientific) using a spectrophotometer (Thermo Scientific Genesys 30).

Gibson assembly was performed using pABG5 as previously described [11]. Transformation of plasmids into *E.coli*, *S. mitis*, and *E.faecalis* was performed as previously described in [11, 16, 54, 55].

4.3 Acidic Bligh-Dyer Lipid Extractions

Bacteria were grown for approximately 16 hours overnight in 15 mL of an appropriate culture medium. After growth, OD_{600nm} measurements were taken, and cells were pelleted at 4,280 x g for 5 minutes at room temperature in a Sorvall RC6+ centrifuge. The supernatant was tipped out, and the cell pellet was washed and resuspended in 1X Phosphate Buffered Saline (PBS). The cells were pelleted again, and all the supernatant was aspirated out. The cell pellet was stored at -80°C until lipid extraction. An acidic Bligh-Dyer lipid extraction was performed as previously reported [16, 12]. Briefly, cell pellets were resuspended in 0.8 mL of 1x Dulbecco's PBS (Sigma-Aldrich). Cells were transferred to a 9 mL glass tube with a Teflon-lined cap (Pyrex). 1 mL chloroform (MilliporeSigma) and 2 mL methanol (Thermo Fisher Scientific) were added to create the single-phase Bligh-Dyer. Tubes were vortexed every 5 minutes for 20 minutes, then centrifuged at 500 x g for 10 minutes at room temperature. The supernatant was transferred to a new 9 mL glass tube. 100 μL of Hydrochloric acid (Thermo Fisher Scientific) was added followed by 1 mL of chloroform and 0.9 mL of 1x Dulbecco's PBS to create the two-phase Bligh-Dyer. Tubes were gently mixed and centrifuged at 500 x g for 5 minutes at room temperature. After centrifuging, the bottom layer was extracted to a new tube and dried under nitrogen gas and stored at -80°C prior to lipidomic analysis. Lipid analyses were repeated in biological triplicate aside, from OG1RF_10760::Tn extractions, which were performed once.

4.4 Analysis of lysine lipids by an amino column-based Liquid Chromatography-Electrospray Ionization-Mass Spectrometry (LC-ESI MS): A new method

An amino column-based normal phase LC-ESI MS was performed using an Agilent 1200 Quaternary LC system coupled to a high-resolution TripleTOF5600 mass spectrometer (Sciex, Framingham, MA). A Unison UK-Amino column (3 μm, 25 cm $\times$ 2 mm) (Imtakt USA, Portland, OR) was used. Mobile phase A consisted of chloroform/methanol/aqueous ammonium hydroxide (800:195:5, v/v/v). Mobile phase B consisted of chloroform/methanol/water/ aqueous ammonium hydroxide (600:340:50:5, v/v/v/v). Mobile phase C consisted of chloroform/methanol/water/aqueous ammonium hydroxide (450:450:95:5, v/v/v/v). The elution program consisted of the following: 100% mobile phase A was held isocratically for 2 min and then linearly increased to 100% mobile phase B over 8 min and held at 100% B for 5 min. The LC gradient was then changed to 100% mobile phase C over 1 min and held at 100% C for 3 min, and finally returned to 100% A over 0.5 min and held at 100% A for 3 min. The total LC flow rate was 300 μl/min. The MS settings were as follows: Ion spray voltage (IS) = 5000 V, Curtain gas (CUR) = 20 psi, Ion source gas 1 (GS1) = 20 psi, De-clustering potential (DP) = 50 V, and Focusing Potential (FP) = 150 V. Nitrogen was used as the collision gas for MS/MS experiments. Data acquisition and analysis were performed using Analyst TF1.5 software (Sciex, Framingham, MA).

4.5 Generation of *mprF* expression plasmids

The *S. downei mprF* nucleotide sequence (Locus tag HMPREF9176_RS03810) and *S. ferus mprF* nucleotide sequence (Locus tag A3GY_RS0106165) were used to design synthetic geneblocks (GeneWiz from Azenta Life Sciences). A 20 nucleotide 5' extension and a 20 nucleotide 3' extension complementary to the pABG5 plasmid were added to enable Gibson assembly of the inserts with pABG5. Sequences for the geneblocks can be found in Table S5. The *S. salivarius mprF* (Locus tag SSAL8618_04345) was amplified from *Streptococcus salivarius* ATCC 7073. A 20 nucleotide 5' extension and a 20 nucleotide 3' extension complementary to the pABG5 plasmid was added to the insert. The same protocol was used for generation of pSobrinus, pEFMprF1, pEFMprF2, and pOGMprF2 with slight modifications. *S. sobrinus mprF* (Locus tag DLJ52_05040) was amplified from *Streptococcus sobrinus* ATCC 27352. *E. faecium mprF1* (Locus tag EFTG_00601) and *E. faecium mprF2* (Locus tag EFTG_02430) were amplified from *Enterococcus faecium* 1, 231, 410. *E. faecalis mprF2* (Locus tag OG1RF_10760) was amplified from *E. faecalis* OG1RF.

4.6 Boltzmann Machines and Restricted Boltzmann Machines for Protein Sequences

Formulation of models

The Boltzmann Machine, as described in [18], is defined as:

$$P(\mathbf{v}) = \frac{1}{Z}\exp\{\sum_{i<j} e_{ij}(v_i, v_j) + \sum_i h_i(v_i)\} \tag{2}$$

which is a probability distribution defined on the pairwise interactions (the couplings e_{ij}) between the positions (v_n) in an input sequence ($\mathbf{v}$) and a local field term h_i. The pairwise coupling matrix is akin to a covariance matrix, and the local fields are similar to single site frequency measures.

The joint probability distribution of the Restricted Boltzmann Machine as described in [14] is as follows:

$$P(\mathbf{v}, \mathbf{h}) = \frac{1}{Z}\exp\left(\sum_{i=1}^{N} g_i(v_i) - \sum_{\mu=1}^{M} \mathcal{U}_\mu(h_\mu) + \sum_{i\mu} h_\mu w_{i\mu}(v_i)\right) \tag{3}$$

Here, the vector $\mathbf{v}$ again represents the input sequence data, $g(v_i)$ is a local field which controls the conditional probability of the input data, $\mathcal{U}_\mu$ is the hidden unit potential/activation, and the terms h_i and $w_{i\mu}(v)$ couple the input variables with the hidden unit variables. In this way, interactions between residues are mediated by a relatively smaller set of hidden units which do not interact directly with each other, leading to a bipartite structure as opposed to the Boltzmann machine's fully connected pair based formulation.

Particularly important is the potential function $\mathcal{U}$, which in this work is the dRELU function defined as:

$$\begin{aligned} \mathcal{U}_\mu(h) =& \frac{1}{2}\gamma_{\mu,+}h_+^2 + \frac{1}{2}\gamma_{\mu,-}h_-^2 + \theta_{\mu,+}h_+ + \theta_{\mu,-}h_- \quad \text{where} \\ & h_+ = \max(h, 0)\ ,\ h_- = \min(h, 0) \end{aligned} \tag{4}$$

The four parameters $\gamma_{\mu,\pm}, \theta_{\mu,\pm}$ are learned through the inference procedure, and allow the positive and negative components of the hidden units w_μ to be separately gated, which allows learning of bimodal distributions for the activations h_μ. Another key feature is the sparsity regularization on the weights applied during model inference:

$$L2/L1 = \frac{\lambda_1^2}{2qN}\sum_\mu \left(\sum_{i,v} |w_{i\mu}(v)|\right)^2 \tag{5}$$

where q is the number of amino acids plus a gap character (21) and the hyperparameter λ_1^2 can be increased to induce sparsity and lower weight magnitude. Equations 4 and 5 together guide the representation of the hidden units to bimodal outputs with interpretable features.

Dataset acquisition and preprocessing

Multiple sequence alignment used for model training was the DUF2156 domain acquired from Pfam [25] (in later revisions renamed LPG_synthase_C). Starting with this MSA, it was processed to include only amino acid characters and gaps, excluding sequences with ambiguous or non-standard characters. Additionally, sequences with contiguous strings of gaps greater than 20% of the full sequence's length were removed. This left 11,507 sequences with a length of 298. After the data cleaning process described in Figure 4, a total of 7,865 sequences were used to train our final model.

Model training

The model previously described [14] was utilized, specifically the Python 2.7 version freely available on Github (`https://github.com/jertubiana/ProteinMotifRBM`). Extensive testing of the combinations of the number of hidden units, $L2/L1$ regularization, and learning rate were performed. Models were trained in triplicate with different random seeds, as the training procedure converges to slightly different weight values depending on their initial random configuration. Training was considered successful when the model consistently produced similar sets of weights across different random seeds, and the weights had the previously mentioned sparsity and magnitude indicating compositional representation. The final model used in this work was trained for 2000 epochs with a learning rate of 0.1, a learning rate decay of 0.33, $L2/L1$ parameter λ_1^2 set to 1.0, and 300 hidden units.

Model Weight selection

To find hidden units which were relevant to function we computed the $L1$ norm of each hidden unit individually, then ranked them. The hidden units with the largest magnitude were looked at first, and these were typically the sparsest of all hidden units. Hidden units were chosen which involved sequence coordinates implicated in our function of interest. Specifically, locations identified through Autodock [26] where the lipid was likely to interact, and a small radius around this region to select a small set of coordinates. We chose the only hidden units which had both overlap with multiple residues in this chosen radius and predictive power (separation) for the three examples we had to start with.

Software Accessibility

DUF2156 domain sequences were retrieved from Pfam33 [25]. Raw sequence datasets are available as Supplementary Material.

5 Acknowledgments

J.M. and F.M. acknowledge support from the National Institutes of Health (NIH R35GM133631). F.M. acknowledges support from the National Science Foundation CAREER award (MCB-1943442). We acknowledge support from the National Institutes of Health grant R01AI178692 (Z.G., F. M. and K.P.) and R01AI148366 (Z.G. and K.P.). K.P. acknowledges support from the Cecil H. and Ida Green Chair in Systems Biology Science. L.R.J acknowledges support from the American Heart Association (23POST1013835)

References

[1] Eoin Fahy, Dawn Cotter, Manish Sud, and Shankar Subramaniam. Lipid classification, structures and tools. *Biochimica et Biophysica Acta (BBA)-Molecular and Cell Biology of Lipids*, 1811(11):637–647, 2011.

[2] Lang-Hong Wang, Xin-An Zeng, Man-Sheng Wang, Charles S Brennan, and Deming Gong. Modification of membrane properties and fatty acids biosynthesis-related genes in escherichia coli and staphylococcus aureus: Implications for the antibacterial mechanism of naringenin. *Biochimica et Biophysica Acta (BBA)-Biomembranes*, 1860(2):481–490, 2018.

[3] Hervé Roy, Kiley Dare, and Michael Ibba. Adaptation of the bacterial membrane to changing environments using aminoacylated phospholipids. *Molecular microbiology*, 71(3):547–550, 2009.

[4] Hervé Roy and Michael Ibba. Rna-dependent lipid remodeling by bacterial multiple peptide resistance factors. *Proceedings of the National Academy of Sciences*, 105(12):4667–4672, 2008.

[5] Christian Sohlenkamp and Otto Geiger. Bacterial membrane lipids: diversity in structures and pathways. *FEMS microbiology reviews*, 40(1):133–159, 2016.

[6] Christopher Weidenmaier, Andreas Peschel, Volkhard AJ Kempf, Natalie Lucindo, Michael R Yeaman, and Arnold S Bayer. Dltabcd-and mprf-mediated cell envelope modifications of staphylococcus aureus confer resistance to platelet microbicidal proteins and contribute to virulence in a rabbit endocarditis model. *Infection and immunity*, 73(12):8033–8038, 2005.

[7] Luke R Joyce and Kelly S Doran. Gram-positive bacterial membrane lipids at the host–pathogen interface. *PLoS Pathogens*, 19(1):e1011026, 2023.

[8] Vipul Gujrati, Sunghyun Kim, Sang-Hyun Kim, Jung Joon Min, Hyon E Choy, Sun Chang Kim, and Sangyong Jon. Bioengineered bacterial outer membrane vesicles as cell-specific drug-delivery vehicles for cancer therapy. *ACS nano*, 8(2):1525–1537, 2014.

[9] Christoph M. Ernst, Petra Staubitz, Nagendra N. Mishra, Soo-Jin Yang, Gabriele Hornig, Hubert Kalbacher, Arnold S. Bayer, Dirk Kraus, and Andreas Peschel. The bacterial defensin resistance protein mprf consists of separable domains for lipid lysinylation and antimicrobial peptide repulsion. *PLOS Pathogens*, 5(11):1–9, 11 2009.

[10] Petra Staubitz, Heinz Neumann, Tanja Schneider, Imke Wiedemann, and Andreas Peschel. Mprf-mediated biosynthesis of lysylphosphatidylglycerol, an important determinant in staphylococcal defensin resistance. *FEMS microbiology letters*, 231(1):67–71, 2004.

[11] Luke R. Joyce, Haider S. Manzer, Jéssica da C. Mendonça, Ricardo Villarreal, Prescilla E. Nagao, Kelly S. Doran, Kelli L. Palmer, and Ziqiang Guan. Identification of a novel cationic glycolipid in streptococcus agalactiae that contributes to brain entry and meningitis. *PLOS Biology*, 20(2):1–15, 02 2022.

[12] Luke R Joyce, Ziqiang Guan, and Kelli L Palmer. Streptococcus pneumoniae, s. pyogenes and s. agalactiae membrane phospholipid remodelling in response to human serum. *Microbiology*, 167(5), 2021.

[13] Christiam Camacho, George Coulouris, Vahram Avagyan, Ning Ma, Jason Papadopoulos, Kevin Bealer, and Thomas L. Madden. BLAST+: architecture and applications. *BMC Bioinformatics*, 10(1):421, December 2009.

[14] Jérôme Tubiana, Simona Cocco, and Rémi Monasson. Learning protein constitutive motifs from sequence data. *eLife*, 8:e39397, March 2019.

[15] Hannah M Adams, Luke R Joyce, Ziqiang Guan, Ronda L Akins, and Kelli L Palmer. Streptococcus mitis and s. oralis lack a requirement for cdsa, the enzyme required for synthesis of major membrane phospholipids in bacteria. *Antimicrobial agents and chemotherapy*, 61(5):e02552–16, 2017.

[16] Luke R Joyce, Ziqiang Guan, and Kelli L Palmer. Phosphatidylcholine biosynthesis in mitis group streptococci via host metabolite scavenging. *Journal of bacteriology*, 201(22):e00495–19, 2019.

[17] P. Smolensky. Information processing in dynamical systems: foundations of harmony theory. *MIT Press*, pages 194–281, January 1986.

[18] Faruck Morcos, Andrea Pagnani, Bryan Lunt, Arianna Bertolino, Debora S. Marks, Chris Sander, Riccardo Zecchina, José N. Onuchic, Terence Hwa, and Martin Weigt. Direct-coupling analysis of residue coevolution captures native contacts across many protein families. *Proceedings of the National Academy of Sciences*, 108(49):E1293–E1301, December 2011.

[19] Ryan R. Cheng, Faruck Morcos, Herbert Levine, and José N. Onuchic. Toward rationally redesigning bacterial two-component signaling systems using coevolutionary information. *Proceedings of the National Academy of Sciences*, 111(5):E563–E571, 2014.

[20] Xian-Li Jiang, Rey P. Dimas, Clement T. Y. Chan, and Faruck Morcos. Coevolutionary methods enable robust design of modular repressors by reestablishing intra-protein interactions. *Nature Communications*, 12(1):5592, September 2021.

[21] Nina M. Goodey and Stephen J. Benkovic. Allosteric regulation and catalysis emerge via a common route. *Nature Chemical Biology*, 4(8):474–482, August 2008.

[22] Matteo Figliuzzi, Pierre Barrat-Charlaix, and Martin Weigt. How pairwise coevolutionary models capture the collective residue variability in proteins? *Molecular Biology and Evolution*, 35(4):1018–1027, Jan 2018.

[23] Jérôme Tubiana, Simona Cocco, and Rémi Monasson. Learning Compositional Representations of Interacting Systems with Restricted Boltzmann Machines: Comparative Study of Lattice Proteins. *Neural Computation*, 31(8):1671–1717, August 2019.

[24] Christoph J Slavetinsky, Andreas Peschel, and Christoph M Ernst. Alanyl-phosphatidylglycerol and lysyl-phosphatidylglycerol are translocated by the same mprf flippases and have similar capacities to protect against the antibiotic daptomycin in staphylococcus aureus. *Antimicrobial agents and chemotherapy*, 56(7):3492–3497, 2012.

[25] Jaina Mistry, Sara Chuguransky, Lowri Williams, Matloob Qureshi, Gustavo A Salazar, Erik LL Sonnhammer, Silvio CE Tosatto, Lisanna Paladin, Shriya Raj, Lorna J Richardson, et al. Pfam: The protein families database in 2021. *Nucleic acids research*, 49(D1):D412–D419, 2021.

[26] Stefanie Hebecker, Joern Krausze, Tatjana Hasenkampf, Julia Schneider, Maike Groenewold, Joachim Reichelt, Dieter Jahn, Dirk W. Heinz, and Jürgen Moser. Structures of two bacterial resistance factors mediating tRNA-dependent aminoacylation of phosphatidylglycerol with lysine or alanine. *Proceedings of the National Academy of Sciences*, 112(34):10691–10696, August 2015.

[27] L. M. Mundy, D. F. Sahm, and M. Gilmore. Relationships between enterococcal virulence and antimicrobial resistance. *Clinical Microbiology Reviews*, 13(4):513–522, 2000.

[28] Yinyin Bao, Tuerkan Sakinc, Diana Laverde, Dominique Wobser, Abdellah Benachour, Christian Theilacker, Axel Hartke, and Johannes Huebner. Role of mprf1 and mprf2 in the pathogenicity of enterococcus faecalis. *PLoS One*, 7(6):e38458, 2012.

[29] Hervé Roy and Michael Ibba. Broad range amino acid specificity of rna-dependent lipid remodeling by multiple peptide resistance factors*. *Journal of Biological Chemistry*, 284(43):29677–29683, 2009.

[30] Jennifer L Dale, Kenneth B Beckman, Julia LE Willett, Jennifer L Nilson, Nagendra P Palani, Joshua A Baller, Adam Hauge, Daryl M Gohl, Raymond Erickson, Dawn A Manias, et al. Comprehensive functional analysis of the enterococcus faecalis core genome using an ordered, sequence-defined collection of insertional mutations in strain og1rf. *Msystems*, 3(5):e00062–18, 2018.

[31] Andreas Peschel, Ralph W Jack, Michael Otto, L Vincent Collins, Petra Staubitz, Graeme Nicholson, Hubert Kalbacher, Willem F Nieuwenhuizen, Günther Jung, Andrej Tarkowski, et al. Staphylococcus aureus resistance to human defensins and evasion of neutrophil killing via the novel virulence factor mprf is based on modification of membrane lipids with l-lysine. *The Journal of experimental medicine*, 193(9):1067–1076, 2001.

[32] Thomas D Schneider and R Michael Stephens. Sequence logos: a new way to display consensus sequences. *Nucleic acids research*, 18(20):6097–6100, 1990.

[33] Frances H. Arnold. Directed Evolution: Bringing New Chemistry to Life. *Angewandte Chemie (International Ed. in English)*, 57(16):4143–4148, April 2018.

[34] Manuel J. Carrasco, Suman Alishetty, Mohamad-Gabriel Alameh, Hooda Said, Lacey Wright, Mikell Paige, Ousamah Soliman, Drew Weissman, Thomas E. Cleveland, Alexander Grishaev, and Michael D. Buschmann. Ionization and structural properties of mRNA lipid nanoparticles influence expression in intramuscular and intravascular administration. *Communications Biology*, 4(1):1–15, August 2021.

[35] Mogens Kilian, LENA MIKKELSEN, and JØRGEN HENRICHSEN. Taxonomic study of viridans streptococci: description of streptococcus gordonii sp. nov. and emended descriptions of streptococcus sanguis (white and niven 1946), streptococcus oralis (bridge and sneath 1982), and streptococcus mitis (andrewes and horder 1906). *International Journal of Systematic Bacteriology*, 39(4):471–484, 1989.

[36] Robin G Taylor, David C Walker, and RR McInnes. E. coli host strains significantly affect the quality of small scale plasmid dna preparations used for sequencing. *Nucleic acids research*, 21(7):1677, 1993.

[37] F Kunst, N Ogasawara, I Moszer, AM Albertini, GO Alloni, Vasco Azevedo, MG Bertero, Philippe Bessières, A Bolotin, Sea Borchert, et al. The complete genome sequence of the gram-positive bacterium bacillus subtilis. *Nature*, 390(6657):249–256, 1997.

[38] Barry N Kreiswirth, Sven Löfdahl, Marsha J Betley, Mary O'reilly, Patrick M Schlievert, Merlin S Bergdoll, and Richard P Novick. The toxic shock syndrome exotoxin structural gene is not detectably transmitted by a prophage. *Nature*, 305(5936):709–712, 1983.

[39] JANE M Kuypers, LAURA M Heggen, and CRAIG E Rubens. Molecular analysis of a region of the group b streptococcus chromosome involved in type iii capsule expression. *Infection and immunity*, 57(10):3058–3065, 1989.

[40] Cristina Faralla, Matteo M Metruccio, Matteo De Chiara, Rong Mu, Kathryn A Patras, Alessandro Muzzi, Guido Grandi, Immaculada Margarit, Kelly S Doran, and Robert Janulczyk. Analysis of two-component systems in group b streptococcus shows that rgfac and the novel fspsr modulate virulence and bacterial fitness. *MBio*, 5(3):e00870–14, 2014.

[41] Brady L Spencer, Anushila Chatterjee, Breck A Duerkop, Carol J Baker, and Kelly S Doran. Complete genome sequence of neonatal clinical group b streptococcal isolate cjb111. *Microbiology resource announcements*, 10(2):e01268–20, 2021.

[42] Kelli L Palmer, Karen Carniol, Janet M Manson, David Heiman, Terry Shea, Sarah Young, Qiandong Zeng, Dirk Gevers, Michael Feldgarden, Bruce Birren, et al. High-quality draft genome sequences of 28 enterococcus sp. isolates. *Journal of bacteriology*, 192(9):2469–2470, 2010.

[43] Shonna M McBride, Vincent A Fischetti, Donald J LeBlanc, Robert C Moellering Jr, and Michael S Gilmore. Genetic diversity among enterococcus faecalis. *PloS one*, 2(7):e582, 2007.

[44] Olga G. Gold, H.V. Jordan, and J. van Houte. The prevalence of enterococci in the human mouth and their pathogenicity in animal models. *Archives of Oral Biology*, 20(7):473–IN15, 1975.

[45] Belle M Sharon, Neha V Hulyalkar, Philippe E Zimmern, Kelli L Palmer, and Nicole J De Nisco. Inter-species diversity and functional genomic analyses of closed genome assemblies of clinically isolated, megaplasmid-containing enterococcus raffinosus er676 and atcc49464. *Access Microbiology*, pages 000508–v1, 2023.

[46] MD Collins, UM Rodrigues, NE Pigott, and RR Facklam. Enterococcus dispar sp. nov. a new enterococcus species from human sources. *Letters in Applied Microbiology*, 12(3):95–98, 1991.

[47] D. B. Drucker. 3: Sweetening agents in food, drinks and medicine: Cariogenic potential and adverse effects. *International journal of food sciences and nutrition*, 33(2):114–124, 1979.

[48] Matthew D Collins, Brian A Phillips, and Paolo Zanoni. Deoxyribonucleic acid homology studies of lactobacillus casei, lactobacillus paracasei sp. nov., subsp. paracasei and subsp. tolerans, and lactobacillus rhamnosus sp. nov., comb. nov. *International Journal of Systematic and Evolutionary Microbiology*, 39(2):105–108, 1989.

[49] PA Hansen and Erwin F Lessel. Lactobacillus casei (orla-jensen) comb. nov. *International Journal of Systematic and Evolutionary Microbiology*, 21(1):69–71, 1971.

[50] Morrison Rogosa and P Arne Hansen. Nomenclatural considerations of certain species of lactobacillus beijerinck: Request for an opinion. *International Journal of Systematic and Evolutionary Microbiology*, 21(2):177–186, 1971.

[51] Frederick Dixon Chester. *A manual of determinative bacteriology*. Macmillan, 1901.

[52] Hannah M Adams, Xiang Li, Carmela Mascio, Laurent Chesnel, and Kelli L Palmer. Mutations associated with reduced surotomycin susceptibility in clostridium difficile and enterococcus species. *Antimicrobial Agents and Chemotherapy*, 59(7):4139–4147, 2015.

[53] Janet M Manson, Stefanie Keis, John MB Smith, and Gregory M Cook. A clonal lineage of vana-type enterococcus faecalis predominates in vancomycin-resistant enterococci isolated in new zealand. *Antimicrobial agents and chemotherapy*, 47(1):204–210, 2003.

[54] Gabriela Salvadori, Roger Junges, Donald A Morrison, and Fernanda C Petersen. Overcoming the barrier of low efficiency during genetic transformation of streptococcus mitis. *Frontiers in microbiology*, 7:1009, 2016.

[55] Brett D Shepard and Michael S Gilmore. Electroporation and efficient transformation of enterococcus faecalis grown in high concentrations of glycine. *Electroporation Protocols for Microorganisms*, pages 217–226, 1995.

Lipid discovery enabled by sequence statistics and machine learning

Priya M. Christensen[1], Jonathan Martin[1], Aparna Uppuluri[1], Luke R. Joyce[4], Yahan Wei[5], Ziqiang Guan[6*], Faruck Morcos[1*, 2, 3], and Kelli L. Palmer[1*]

[1]Department of Biological Sciences, University of Texas at Dallas, Richardson, TX 75080, USA
[2]Department of Bioengineering, University of Texas at Dallas, Richardson, TX 75080, USA
[3]Center for Systems Biology, University of Texas at Dallas, Richardson, TX 75080, USA
[4]Department of Immunology and Microbiology, University of Colorado Anschutz Medical Campus, Aurora, CO 80045, USA
[5]School of Podiatric Medicine, University of Texas Rio Grande Valley, Harlingen, TX 78550, USA
[6]Department of Biochemistry, Duke University Medical Center, Durham, NC 27710, USA

August 19, 2024

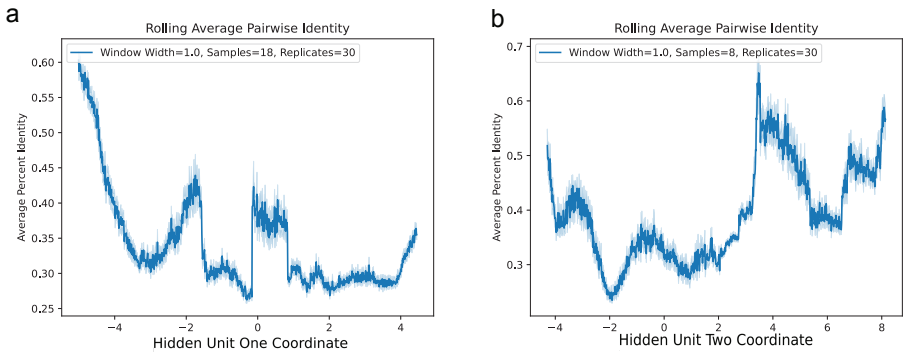

Figure S1: Assessment of RBM hidden unit's reliance on total sequence identity in classification. A sliding window average is performed, where a window of width 1 is slid from the negative end to the positive of the hidden unit activation, where at each position sequence coordinates are sampled from the window. These sampled sequences are compared pairwise between themselves, computing the Hamming distance across their entire sequence length to produce an average. This sampling procedure is repeated 30 times for each window, with the light blue shading representing the 95% confidence interval.

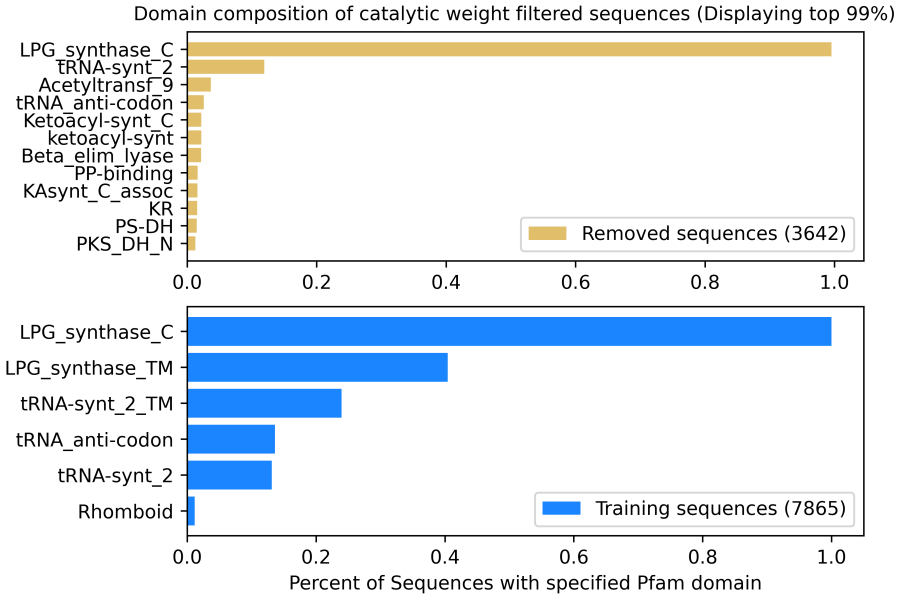

Figure S2: The full sequences of our pre-filtered multiple sequence alignment were analyzed to identify which Pfam domains were present in them. We then split these results based on the procedure in Figure 3, where Removed sequences indicate domain composition of sequences removed by this procedure, and Training sequences for the data we trained our final model on. We remove domains from this plot which occur in less than 1% of the sequences of their respective sets for clarity.

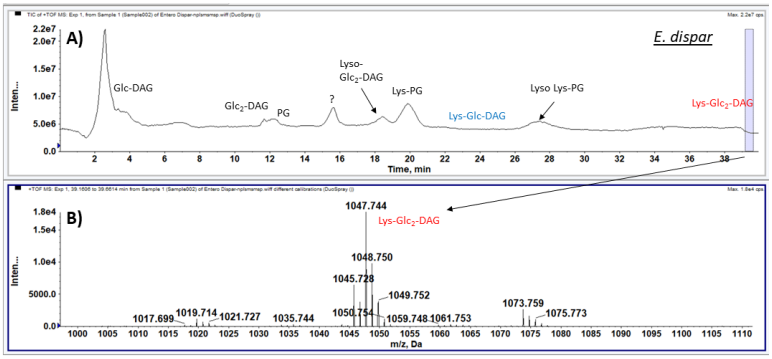

Figure S3: Identification of Lys-Glc$_2$-DAG which is highly retentive on a silica HPLC column. A) the total ion chromatogram of normal phase LC/MS of *E. dispar* lipids separated on a silica HPLC column. B) the positive ion mass spectrum of Lys-Glc$_2$-DAG eluting at the end of the LC gradient. Glc-DAG, glucosyl-diacylglycerol; Glc$_2$-DAG, diglucosyl-diacylglycerol; PG, phosphatidylglycerol; Lyso-Glc$_2$-DAG, lyso diglucosyl-diacylglycerol; Lys-PG, lysyl-phosphatidylglycerol; Lys-Glc-DAG, lysyl-glucosyl-diacylglycerol; Lyso Lys-PG, lyso lysyl-phosphatidylglycerol; Lys-Glc$_2$-DAG, lysyl-diglucosyl-diacylglycerol.

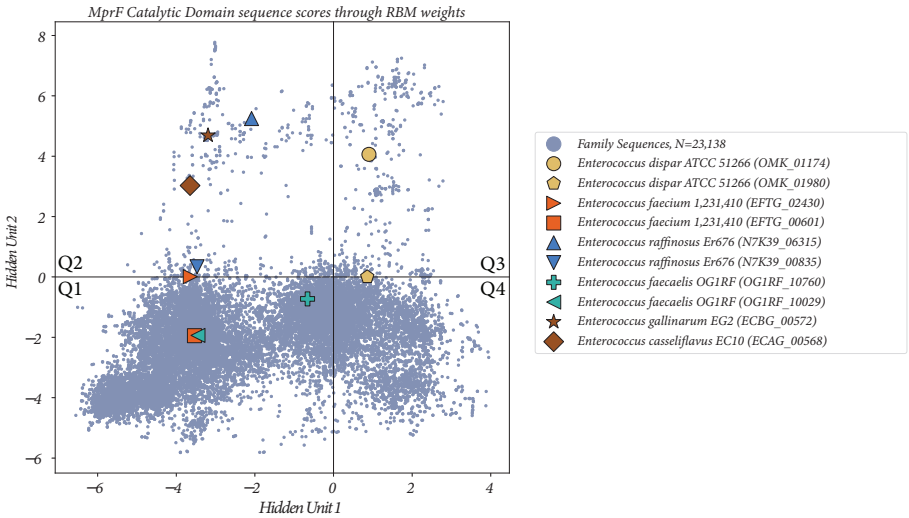

Figure S4: All *Enterococcus* sequences analyzed in the course of this study.

Bacterial Strain	Protein ID	Locus ID	Description	Reference
Enterococcus dispar ATCC 51266 *(mprf1)*	WP_016173119	OMK_01174	Wild-type *E. dispar* strain	Collins et al. (1991)
Enterococcus dispar ATCC 51266 *(mprf2)*	WP_016172352	OMK_01980	Wild-type *E. dispar* strain	Collins et al. (1991)
Enterococcus gallinarum EG2	WP_195971496	ECBG_00572	Wild-type *E. gallinarium* strain	Palmer et al. (2010)
Enterococcus casseliflavus EC10	WP_201705909	ECAG_00568		Palmer et al. (2010)
Enterococcus faecalis T11 *(mprF1)*	EEU90403	EFMG_00309	Wild-type *E. faecalis* strain	McBride et al. (2007)
Enterococcus faecalis T11 *(mprF2)*	EEU90403	EFMG_01835	Wild-type *E. faecalis* strain	McBride et al. (2007)
Enterococcus faecalis OG1RF *(mprf1)*	WP_002414160	OG1RF_10029	Wild-type *E.faecalis* strain	Gold et al. (1975)
Enterococcus faecalis OG1RF *(mprf2)*	WP_002358907	**OG1RF_10760**	Wild-type *E.faecalis* strain	Gold et al. (1975)
Enterococcus faecium 1,231,410 *(mprf1)*	WP_002294379	**EFTG_00601**	Wild-type *E. faecium* strain	Palmer et al. (2010)
Enterococcus faecium 1,231,410 *(mprf2)*	WP_002287340	EFTG_02430	Wild-type *E. faecium* strain	Palmer et al. (2010)
Enterococcus raffinosus Er676	UXJ96875	N7K39_06315	Wild-type *E. raffinosus* strain	Sharon et al. (2023)
Streptococcus agalactiae COH1	CDN67397	GBSCOH1_1931	Wild-type *S. agalactiae* strain, serotype III	Kuypers et al. (1989)
Streptococcus agalactiae CJB111	QOW76674	ID870_10050	Wild-type *S.agalactiae* strain, serotype V	Faralla et al. (2014); Spencer et al. (2021)
Staphylococcus aureus RN4220	QWF27327	NMK49_RS06325	Wild-type *S. aureus* strain	Kreiswirth et al. (1983)
Bacillus subtilis 168	QJF41380	BSU_08425	Wild-type *B. subtilis* strain	Kunst et al. (1997)
Bacillus licheniformis ATCC 14580	WP_003179900	EJ992_04410	Wild-type *B. licheniformis* strain	Chester (1901)
Exiguobacterium acetylicum UTDF19-27C	WP_238238782	K6T22_02680	Wild-type *E. acetylicum* strain	
Ligilactobacillus salivarius ATCC 14580	EEJ74510	HMPREF0545_0714	Wild-type *L. salivarius* strain	Drucker (1979)
Lacticaseibacillus rhamnosus ATCC 7469		NHLLHDLP_02198	Wild-type *L. rhamnosus* strain	Collins et al. (1989)
Lactobacillus casei ATCC 393	BAN75198	LBCZ_2030	Wild-type *L. casei* strain	Hansen and Lessel (1971)
Levilactobacillus brevis ATCC 14869	ERK41244	HMPREF0495_02376	Wild-type *L. brevis* strain	Rogosa and Hansen (1971)
Lacticaseibacillus paracasei ATCC 25302	TDG89985	C5L26_003005	Wild-type *L. paracasei* strain	Collins et al. (1989)
Streptococcus mitis SM61 + pFerus	WP_018030543	A3GY_RS0106165	Exprssion of *S. ferus mprF* in *S. mitis*	This work
Streptococcus mitis SM61 + pDownei	WP_002997695	HMPREF9176_1523	Expression of *S. downei mprF* in *S.mitis*	This work
Streptococcus mitis SM61 + pSobrinus	WP_019781626	DLJ52_05040	Expression of *S. sobrinus mprF* in *S. mitis*	This work
Streptococcus mitis SM61 + pSalivarius	WP_181671155	SSAL8618_04345	Expression of the *S. salivarius mprF* in *S.mitis*	This work
Enterococcus faecalis OG1RF_10760::Tn			OG1RF with a mini-mariner transposon (EfaMarTn) inserted into MprF2 at position 787608	Dale et al. (2018)
Enterococcus faecalis OG1RF_10760::Tn + pABG5	WP_002358907	OG1RF_10760	OG1RF_10760::Tn with the empty vector pABG5 expressed	This work
Enterococcus faecalis OG1RF_10760::Tn + pOGMprF2	WP_002358907	OG1RF_10760	Complementation of the transposon. pOG_MprF2 expresses the OG1RF_10760 gene on the pABG5 vector	This work
Enterococcus faecalis OG1RF_10760::Tn + pEfMprF1	WP_002294379	EFTG_00601	Expression of MprF1 from *E. faecium* 1, 231, 410 into the OG1RF_10760::Tn	this work
Enterococcus faecalis OG1RF_10760::Tn + pEfMprF2	WP_002287340	EFTG_02430	Expression of MprF2 from *E. faecium* 1, 231, 410 into the OG1RF_10760::Tn	this work

Table S1: Sequence Locus IDs for all sequences listed in Table 2. Bold denotes confirmed *mprF* allele.

Table S2: Fisher's exact test for determining whether positive values of Hidden Unit 2 are predictive of Glc_N-DAG specificity. p=0.028.

	Hidden Unit 2 Positive	**Hidden Unit 2 Negative**
Glc_N-DAG	8	4
PG Only	1	7

E.coli and Plasmid	Description	Reference
E.coli DH5α (pFerus)	*E. coli* with *S. ferus mprF* in pABG5	This Study
E.coli DH5α (pDownei)	*E. coli* with *S. downei mprF* in pABG5	This Study
E.coli DH5α (pSalivarius)	*E. coli* with *S. salivarius* ATCC 7073 *mprF* in pABG5	This Study
E.coli DH5α (pSobrinus)	*E. coli* with *S. sobrinus* ATCC 27352 *mprF* in pABG5	This Study
E.coli DH5α (pEFmprF1)	*E. coli* with *E. faecium mprF1* (EFTG_00601)	Joyce et al. (2022)
E.coli DH5α (pEFmprF2)	*E. coli* with *E. faecium mprF2* (EFTG_02430) in pABG5	This Study
E.coli DH5α (pOGMprF2)	*E. coli* with *E. faecalis mprF2* (OG1RF_10760) in pABG5	This Study
E.coli DH5α (pABG5)	*E. coli* with the empty vector (pABG5)	Joyce et al. (2022)

Table S3: *E.coli* and plasmids used

Primer Name	Sequence	Use	Reference
pABG5-5'	GGAAAGGGACCTCTCTTCCTAAAC	Linearize pABG5 with pABG5-3'	Joyce et al. (2022)
pABG5-3'	GATAAAGGTATTGGTAAATAACAAA	Linearize pABG5 with pABG5-5'	Joyce et al. (2022)
Faec_MprF1_F	GAGAGGTCCCTTTCCTTGTTAAAAAATACCATACAATG	Primer for amplification of *E. faecium mprF*1 with Faec-MprF1_R contains complementary sequence to pABG5 for Gibson assembly	Joyce et al. (2022)
Faec_MprF1_R	ACCAATACCTTTATCTTAATACTTTCTTCGTATCC	Primer for amplification of *E. faecium mprF*1 with Faec_MprF1_R	Joyce et al. (2022)
Faec_MprF2_F	GAGAGGTCCCTTTCCGTGAAAAATAAACGATACTTG	Primer for amplification of *E. faecium mprF*2 with Faec-MprF2_R contains complementary sequence to pABG5 for Gibson assembly	This Study
Faec_MprF2_R	ACCAATACCTTTATCTTATAATTCTGTGAGCACTTC	Primer used for amplification of *E. faecium mprF*2 with Faec-MprF2_R	This Study
OG1RF_MprF2_F	GAGAGGTCCCTTTCCATGAAACAAATTATTCATTGGATC	Primer used for amplification of *E. faecalis mprF*2 with OG1RF_MprF2_R	This Study
OG1RF_MprF2_R	ACCAATACCTTTATCTTAGTCAATATTTTTTTGATCGAC	Primer used for amplification of *E. faecalis mprF*2	This Study
SalMprF_R	ACCAATACCTTTATCCTATTTCCAAAGACGTC	Primer used for amplification of *S. salivarius mprF* with SalMprF_F	This Study
SalMprF_F	GAGAGGTCCCTTTCCATGAAGCGTCTTTTAGAG	Primer used for amplification of *S. salivarius mprF*	This Study
SobMprF_F	GAGAGGTCCCTTTCCTTGAAAGCCGTTCTTG	Primer used for amplification of *S. sobrinus mprF* with SobMprF_R	This Study
SobMprF_R	ACCAATACCTTTATCTTAATTCCGAGTCACAC	Primer used for amplification of *S. sobrinus mprF*	This Study
EF1_S1	GAATAACGCTGATCAAAAGT	Primer used for sequencing pEFMprF1 insert with pABG5Fup2	Joyce et al. (2022)
EF1_S2	TGCCAAGAGAAATAGTC	Primer used for sequencing pEFMprF1 insert with EF1_S3	Joyce et al. (2022)
EF1_S3	ACAATCTCTTCGCTTG	Primer used for sequencing pEFMprF1 insert	Joyce et al. (2022)
EF1_S4	CCAACTGTTCTTCTCCAA	Primer used for sequencing pEFMprF1 insert with pABG5Fdown2	Joyce et al. (2022)
EF2_S1	CTCCTGTATGTGTGATGAAC	Primer used for sequencing pEFMprF2 insert with pABG5Fup2	This Study
EF2_S2	GGAATGGGGACTTTTGA	Primer used for sequencing pEFMprF2 insert with EF2_S3	This Study
EF2_S3	ACTGATTCGTTGCTGC	Primer used for sequencing pEFMprF2 insert	This Study
EF2_S4	CTTCGCTTGTCAGGTTAC	Primer used for sequencing pEFMprF2 insert with pABG5Fdown2	This Study
OG2_S1	TTGTAAAGAACAAACAGCC	Primer used for sequencing pOG_MprF2 insert with pABG5Fup2	This Study
OG2_S2	GCAACTTAGGTGTCG	Primer used for sequencing pOG_MprF2 insert with OG_S3	This Study
OG2_S3	GCCGAAACGATCTGT	Primer used for sequencing pOG_MprF2 insert	This Study
OG2_S4	CGTTGTGATGGGCAAC	Primer used for sequencing pOG_MprF2 insert with pABG5Fdown2	This Study
Sal_S1	GAAGGGAATAACGTAG	Primer used for sequencing pSalivarius insert with pABG5Fup2	This Study
Sal_S2	TATCTTCTCTATGATTCC	Primer used for sequencing pSalivarius insert with Sal_S3	This Study
Sal_S3	TCTTCAAGAAAGATTCCCA	Primer used for sequencing pSalivarius insert	This Study
Sal_S4	CTCTTTTGGTATCGTGTC	Primer used for sequencing pSalivarius insert with pABG5Fdown2	This Study
Sob_S1	AGGAATGACATAATAAGCCAAG	Primer used for sequencing pSobrinus insert with pABG5Fup2	This Study
Sob_S2	CGGTATTATTTCTCTGAT	Primer used for sequencing pSobrinus insert with Sob_S3	This Study
Sob_S3	TTCTACATCGGCCTCAT	Primer used for sequencing pSobrinus insert	This Study
Sob_S4	TTAGCCTTTCTGGGAGAC	Primer used for sequencing pSobrinus insert with pABG5Fdown2	This Study
Downei_S1	GAACATAATAGGCCAGGC	Sequencing primer for pDownei insert with pABG5Fup2	This Study
Downei_S2	CGGTGGGGATTATTTCC	Sequencing primer for pDownei insert with Downei_S3	This Study
Downei_S3	CTGCTTGGTTACCAGCAG	Sequencing primer for pDownei insert	This Study
Downei_S4	CAAACGCCTCTTCTG	Sequencing primer for pDownei insert with pABG5Fdown2	This Study
Ferus_S1	CCGGCAAAGAATGGCAGAATA	Sequencing primer for pFerus insert with pABG5Fup2	This Study
Ferus_S2	CACTAATCCCTGGCGG	Sequencing primer for pFerus insert with Ferus_S3	This Study
Ferus_S3	CAATGAAGGCTCTTGTAGC	Sequencing primer for pFerus insert	This Study
Ferus_S4	GTATCAGGAGGAGGGAC	Sequencing primer for pFerus with pABG5Fdown2	This Study
pABG5Fup2	CAAAAGGTTTCGACTTTTCACC	Primer used for sequencing with pABG5Fup2	Joyce et al. (2022)
pABG5Fdown2	CCAATAATAATGACTAGAGAAG	Primer used for sequencing	Joyce et al. (2022)

Table S4: Primers used in this study. Red indicates sequence complementarity to pABG5.

Name	Sequence
S. Downei mprF (Locus tag HMPREF9176_RS03810)	AGGAAGAGAGGTCCCTTTCC TTGAAAGCCCTTCTTGAAAAAATCAAGCCCCTTACCTCCATTCTTAAA ACCGTCTTCTTTGTTTCCATCATCCTCTTAATCATCATGGAAATCCTCAATCTGAGGCGGACCATTTCTGTGTCGCAACTCAAGG CGGCATTGGGTGGGGTGTCTCCTATCAATATTCTCCTGATTTTTATCATTGGAGCCCTGGCCGTCCTACCAACGACGGGCTATGA TTTTGTCCTCAATAAAATTTTGGGTACCAATAAGTCCAAGTGGTATATTTTGCAGACCTCCTGGTGTATCAATACCTTTAATAAT TTATCGGGTTTTGGCGGTCTGATTGATATTGGTCTGCGTTTGGCCTTCTACGGGCAAAAAGGAGAAGAGGAGCGCGACCTCCAGC AGGTCACGACCTTCCTCCCTTATCTGATTTCGGGCTTGTCCTTTGTCAGTCTGGCTTCTCTGGGTCTGACCTACGCCTATGGAGT CAACCGCTCTGGTCTTCCCTATTATGATATTGTTCTGATTGGAGCTAGTCTCTATTTTCCTATTCTCTATTGGTTGACGGGACGC AAGACCAAGAATTACTTTGCCAATATGCCTGTCAAGACCAGGAACCGTCTAGGGATTGTGTCCTTCTTCGAGTGGTCTTGTGCAG CGGCAGCCTTTATCATTATTGGCCGTCTGATGGGCATTGATATGCCGATTTCCGTCGTTCTGCCCTTCTTTGCCATTGGTTGTGC GGTGGGGATTATTTCCTTGATTCCTGGGGCTCTAGGGAGTTTTGACTTTGTCGTCCTGACAGGTCTGTCTGCCCACGGTTTGCCT AAGGAAACGGTTCTAGCCTGGCTCTTGCTTTACCGCCTGGCCTATTATGTTCTCCCTTTCTTTGTCGGGATTATTTTCTTTATCA GACATCTGGGTGGAAAGATTAATGAGAAATACAATGCCGTTCCCAAGCAGATGCTGGAAAGGGGCATTCATACAGTCACTATCCG TCTGATTCGCTGGTTGGGGATTTTCCTAGCCCTTTCCACCGTCTTCTTTGAAAATCTGGATTATATCACCTGGCTAAGGCCTTTT AACCCCTTGCAGAAGCAGATTATTTGGCAATTTCCAGGTCTCTTGTTGGGGATTTGTTTCATTCTTCTAGCCAGGACCATCGAAA AGAAGGTCAAGCTGGCCTATCCTCTGACCATGATTTGGTTGGTCCTGACTCTGATTTATGTCGATTTTGGAGCTATTAGTTGGGG CTTTTCCATCGCCATTTTCTTAGCTATAATTGCCCTCAATTTGGTTCGACCTCAGCTCTATAAGAAGCAGTTTATTTATTCCTGG GAGGCTAGAACCAAGGATAGCCTGATTATTGCTCTGACCCTGCTTGTGATTTTCACCTTGGCTGGAGTGATTTTCCCTGTTCGGG CCCATGAGCTCCATGAACTCGTGGAGCGGCATAAACCCATCAGTCCAGAAAGCTACCTCCTAACGCGGAAAATCGTTTTAATCAT TACGGTGATTATCACGGTCTCTTACTGGATTTTGATGCGGATTGTTCAAGGACGCAAGGTTAAGTTGGGCACGCCCTTCCAGGCT GACCGCTACCGTAAGCTCCTGGAAACCTATGGTGGTCAAGGGGATAGCGCACTTGCTTTTCTAGGTGACAAACGCCTCTTCTGGT ATCAAAAGGAAGGCGAAGACCGGGTTGCCTTTCAATTCGCTATCCGCAACAACAAATGTCTGGTGATGGGCCAACCTGCTGGTAA CCAAGCAGATGTGGAAGAAGCGATTGCTTATTTCATTGATAAGGCCGATCGGCTGGATTACGACTTGATTTTCTATAGTATCGGT CAAAAGATGACCCTCTACCTGCATGAATTCGGCTTTGAATTTATGAAGGTGGGGGAAAACGCCCTAGTGGATTTGGAAAAATTCA CCCTCAGGGGCAATAAATACAAGCCTTTCCGCAATGCCCTCAATCGGGTGGAGAAGGATGGCTTTAGCTTTGAAGTCTTGGCCAG CCCCCATAGTCCTGAGCTTTTGGCGGAAGTCAAGGCCGTTTCTGACATCTGGCTGGACGGTCGATCTGAAAAGGGCTTCTCACTA GGTTATTTTGACCAGGCCTACTTGCAGGAAGCTGCTCTGGCAGTCGTTCGCAATCAGGAGGGCAAACTGGTTGCCTTTGCCAATG TCATGCCTAATTATCAGGAAAATATCGCTTCCATTGATATGATGCGCTATGACAAGGAGGCCATTCCAAACGGGGTCATGGACTA CCTCTTTATTTCCCTCTTTGTCTATTTCCGAGACCAAGGTATCGGTTATTTCGACTTGGGCATGGCTCCCCTATCAGGAGTTGGT CAGGTCGAGGAAAGCTTTATTCAAGAGCGTTTGGCCTATCTGGTCTATCATTTTGGCAGTCATTTTTACTCCTTTGAAGGTCTTT ATCGCTATAAGGAAAAATTCACCCCACTTTGGGACCAGCGGCTATATTTCCTATTCTAGAACTTCCTGGGTCGGCTATGTCCTTAT GACCCTAGTCTTAGAGGACCGAGTGACCAGAAGTTAA GATAAAGGTATTGGTAAATA
S. ferus mprF (Locus tag A3GY_RS0106165)	AGGAAGAGAGGTCCCTTTCC AGGAAGAGAGGTCCCTTTCCTTGAAAACGATTATTGAGAAACTGAAG GCTTTTATGCCTATCATTAAGGTCATTTTTTTCACCTCAATCGTGGTCTTAATCATTGTTGAGTTAATGCACCTGAAACAAACC ATATCGGTCAAAGAGTTGGGGCAGGTGCTGCAAGGTATTTCTTGGCTTAATATCTTTCTGATTTTTTTAGTCGGCACGCTGGCC GTCTTTCCAACCACAGGATATGATTTCATTGTCAACAGGATTCTAAAAACCAACCACAGCAAATCCTATATTCTGCAGACCAGC TGGTGTATCAATACCTTTAATAATCTGACTGGTTTTGGGGGAATTATTGACATTGGCCTGCGACTTGCCTTTTACGGCAAAAAA GGCGAGGAAGAAAGGGAATTGCAGGAAGTTACCCGTTTTCTGCCCTATCTTATTTCAGGGCTGTCCTTTATCAGCCTTGTTTCC CTAGGATTGGTTTCGATCTTTCCCGTCACAAGGAGTGTCCGTTTTTACGATATCATCCTTTTGGCATCAACCCTTTATTTCCCT CTGATTTATTGGTTTTCCGGCAGAAAAAACAATCACTACTTTGGCAATATGCCCGCAAAAATCCGGCTGCAGCTTGGTCTTGTC TCCCTCTTTGAATGGACTTGTGCGGCGCTTGCTTTTATCATCATTGGCTATCTGATGGGAATTGATTTGCCCTTCTATAAAACG CTACCCCTCTTTAGTATCGCCTGTGCTGCAGGGATTGTGTCACTAATCCCTGGCGGGTTGGGAAGTTTTGAACTGGTCTTGTTT ACCGGCTTTGCTGCCGAAGGCTTGCCCAAAGAAACAGTCGTTGCCTGGCTCTTACTCTATCGTCTGGCTTATTATATTCTGCCA TTCTTTGCCGGTATTTATTTCTTTGTCCGCCATCTTGGACATCAGATTAATCAAAGGTATCAAGGGGCTCCTAGGGAGCTCCTC TCAAGCAGTCTACACAGTGTCATGATACACGCTGTTAGGTGGCTGGGAATCTCACTTGTCTTTTCAACCCTCTTTTTTGAAAAG ATCTCTCATCTCAGCTGGCTAGACGGTTTTGGTCCCTTACAAAAACAGCTTATCTGGCAATTCCCAGGGCTTTTAATCGGGGTT TGCTTTATCCTGCTGGCCAGAGCCATTGCTAATGGGGTTAAGAGGGCTTATTCTCTTATGTTTTTGGGTCTGGCAGCAACCCTT GTGTACATTAATACTGGATCTATCAGTTGGCAATGGTCACTCGCTATTGTCTTACTTGGATTGGGGACTGTCCTTATCCGAACA CACCTCTATAAAGCCCAATTTATCTATTCCTGGGAAGGACGCACCAAAGATATCATCTTGATTTCCTCCATGCTCTTTATCTTA TTCACCCTTGCCAGTCTGATTTTCCCATACCGAGCCTATGAAATGAATCAGCACCTTGGCTTCTCTCGTTACTTTTTGACGTGG AAACATATCCTGCTGGCGACCAGCTTGGTCACCCTAGCCTATGCCTGTCTGGTTAGGTATCTCTACGGTGGTAAAACTTTATTG GGTGAGACTTTTGAGCACGATCGCTACCAGCGTTTATTGAGCGAATATGGCGGCAGCGCCGACAGCGGACTCGCCTTTATAAAA AACAAGCGTCTCTTCTGGTATCAGGAGGAGGGACTTGACAAGGCAGCCTTCCAATTTTCAACTATCAATAACAAGGCTGTTGTC ATGGGAGAGCCGGCTGGAAATCCGGAAACCTTTAAAAATGCTACAAGAGCCTTCATTGAAGCTGCTGATCGCCTCAATTATGAC CTCGTCTTTTACAGTATCGGCAAAGATATGACCCTCTTTTTGCATGAATATGGCTTTGAATTCATGAAAGTGGGGGAAAATGCC CTAGTTGATTTAGATAGCTTCCATCTTAAAGGTAATAAATACAAGCCTTTCCGAAACGCTCTCAACCGTGTTCAAAAAGAAGGA TTCACCTTTGAAATAAGTCCTCAGCCTCACTCGAAAGTCTTATTAGATGAACTAGAGACTATTTCAAACAAATGGCTGGAAAAA AGACAGGAAAAAAGATTCTCACTCGGTTTCTTTGATAGAGACTATTTCCAAGAGGCACCGCTGGCGCTGGTTAAAAATAAGGAA CAGGAAATTGTTGCCTTTGCCAATATTATGCCCAATCACCAGAACGGTATCGTCTCCATCGACTTGATGCGCTACGATGCCAAA AAAATTCCAAATGGGGTCATGGACTACCTCTTCTTATCTCTTTTTATCCATTTTAAGGAAGAAGGACTGGCCTACTTTGACCTT GGAATGGCACCCTTGTGGGGGGTTGGGCAAGTCAAGGAAAGTTTCCTCCACGAACGGCTGGCCTATCTGCTCTACAATTTCGGA ACCCATTTTTATTCCTTTGAAGGACTGCACCAGTACAAAAAGAAATTCAACCCGATTTGGGAGGAACGCTATGTCTCTGTTGCC AAATCCTCTTGGCTGCTCTACGCCATCTTGGGCATTTTCTTACTGGATACCAAACTGTTTAACAAAAAAAGAAGATCCTCTTAG GATAAAGGTATTGGTAAATA

Table S5: *mprF* sequences synthesized by Genewiz. Red indicates sequence complementarity pABG5.